IEEE Access
Multidisciplinary | Rapid Review | Open Access Journal

Received 28 June 2024, accepted 31 July 2024, date of publication 5 August 2024, date of current version 13 September 2024.

Digital Object Identifier 10.1109/ACCESS.2024.3438266

METHODS

A Framework for Qualitative Analysis of Voltage Stability Indices (VSIs)

LOKESH KUMAR YADAV[1], MITRESH KUMAR VERMA[2], (Senior Member, IEEE), PUNEET JOSHI[1], SANJAY AGRAWAL[1], (Member, IEEE), MAJED A. ALOTAIBI[3], HASMAT MALIK[4,5], (Senior Member, IEEE), FAUSTO PEDRO GARCÍA MÁRQUEZ[6], AND MOHAMMAD ASEF HOSSAINI[7]

[1]Electrical Engineering Department, Rajkiya Engineering College Ambedkar Nagar, Akbarpur, Uttar Pradesh 224122, India
[2]Electrical Engineering Department, IIT (BHU) Varanasi, Varanasi, Uttar Pradesh 221005, India
[3]Department of Electrical Engineering, College of Engineering, King Saud University, Riyadh 11421, Saudi Arabia
[4]Department of Electrical Power Engineering, Faculty of Electrical Engineering, Universiti Teknologi Malaysia (UTM), Johor Bahru 81310, Malaysia
[5]Department of Electrical Engineering, Graphic Era (Deemed to be University), Dehradun 248002, India
[6]Ingenium Research Group, Universidad de Castilla-La Mancha, 13071 Ciudad Real, Spain
[7]Department of Physics, Badghis University, Badghis 3351, Afghanistan

Corresponding authors: Majed A. Alotaibi (MajedAlotaibi@ksu.edu.sa), Hasmat Malik (hasmat.malik@gmail.com), and Mohammad Asef Hossaini (asef.hossaini_edu@basu.edu.af)

The authors extend their appreciation to the Researchers Supporting Project at King Saud University, Riyadh, Saudi Arabia, for funding this research work through the project number RSP2023R278.

ABSTRACT Voltage stability assessment (VSA) is invariably an essential step in the satisfactory operation of power system. For this, several Voltage Stability Indices (VSIs) based on 1) Existence of solution for voltage equations, 2) Maximum power transfer (MPT) through a line, 3) MPT theorem/maximum loadability limit, 4) P-V curve, 5) Energy function and 6) Jacobian matrix can be found in the literature. VSIs assist in identifying weak lines and buses, voltage collapse proximity, maximum loadability, voltage stability margin, and prompting countermeasures against voltage instability. This article examines 78 different VSIs based on their concepts, assumptions, thresholds, and formulae. Additionally, mathematical proofs for 29 indices have been elaborated upon so that researchers may familiarize themselves with the underlying concepts of the other existing indices and find newer indices in modern power systems composed of intermittent power generation and dynamic loads. Also, a novel qualitative comparative analysis of VSIs is tabulated. Further, a novel framework has been proposed to aid researchers in shortlisting VSIs for a particular application. This article intends to serve as a meaningful reference to various researchers and individuals working in domains like Distributed Generation (DG) placing and rating, Voltage Stability Assessment (VSA), and power system planning.

INDEX TERMS Voltage stability assessment (VSA), phasor measurement unit, voltage stability index, voltage stability margin, weak bus/line.

LIST OF SYMBOLS AND ABBREVIATIONS

CIGs, converter interfaced generation; MPT, maximum power transfer; FACT, flexible AC transmission; HVDC, high voltage direct current; kW, kilowatt; MW megawatt; V_1, V_2, voltages at the sending and receiving nodes; P_1, Q_1, sending node Watts and VAr power; P_2, Q_2, receiving node Watts and VAr power; S_1, S_2, apparent power at both nodes; ∂_1, ∂_2, voltage angle at both nodes; Y, R/r, X/x, θ, line admittance, resistance, reactance and impedance angle; ∂, voltage angle difference; B_{12}, line susceptance; A, α, B, β, line parameters; ϕ, load impedance angle; I_{cc}, short circuit current; V_{th}, Z_{th}, Thevenin's voltage and impedance respectively; Z_{ii}, Z_i, Thevenin's equivalent impedance of n-bus system; P_l, Q_l, active and reactive power loss respectively; P_{lmax}, Q_{lmax}, maximum active and reactive power loss respectively; $P_{2(max)}$, $Q_{2(max)}$, $S_{2(max)}$, maximum receiving end active, reactive and apparent power; P_{margin}, Q_{margin},

The associate editor coordinating the review of this manuscript and approving it for publication was Feiqi Deng.

S_{margin}, active, reactive and apparent power margin between maximum and actual value respectively; S_{cr}, apparent power at critical point; ∂_{max}, maximum voltage angle difference; ΔV_i, voltage drop at i^{th} bus; β, correction factor; $\hat{Z}_k$, k^{th} bus impedance of adjoint network; $\hat{Z}_{th}$, Thevenin's impedance of adjoint network; I_k, V_k, current and voltage of k^{th} bus; ΔI_k, ΔV_k, current and voltage of k^{th} bus for incremented network; α, arbitrary value more than unity; SGP, sensitivity of active power generated to active power demand; SGQ, sensitivity of active power generated to reactive power demand; λ, system parameter; F_{ij}, element of matrix F; m_1, m_2, sending & receiving bus; Y_s, node specification vector; Y(a), singular vector in the space of Y; J_c, conservative measure of power system (PS) steady state stability; J_0, Jacobian corresponds to the most stable PS state; A_i, Jacobian matrix at given time t_i; λ_i, load margin at given time t_i; ΔC, increase in active power; Δl, increase in load; n, normal vector; I_P, MW dispatch power; I_Q, MVar, dispatch power; B_{ii}, susceptance; w_1, w_2, weights; J_R, reduced Jacobian matrix; v(t), bus voltage; v(0), voltage at bus before contingency; V_s, steady state voltage; β_{i0}, angle between active & reactive power flow gradient; P_{n0}, initial load; P_{maxn}, load at nose point of PV curve; v_d, voltage drop; σ, switching function; d_i, percent diversity; Δt, subinterval; V_L, lower voltage limit; V_t, operating point voltage; P_{ci}, collapse active power; λ_{ci}, maximum coefficient; G_p, conductance of the line; SCC, short circuit capacity; SCC_p, practice SCC; SCC_{min}, minimum SCC; V_{thx}, V_{thy}, real & imaginary part of Thevenin's voltage.

I. INTRODUCTION

Voltage instability is a phenomenon that mainly occurs in heavily loaded networks due to various causes such as difficulty in transmission of reactive power, high reactive power consumption in the network, reverse operation of ON load tap changers (OLTC), cascaded tripping of lines and outage of other elements such as generators, transformers. Usually, Voltage instability is a localized effect [1]. However, repercussions of voltage instability may sometimes affect large part of the system leading to complete blackout. Voltage collapse or blackout are typically the outcome of chronologically occurring events associated with voltage instability that may lead to lower voltage profile in significant parts of the power system network [2], [3].

Voltage stability has been studied through different indices. Earlier research concentrated on offline studies through voltage stability indices. With advent of phasor measurement units (PMUs) it has become possible to maintain voltage stability of the system in real time framework. Many indices that have been used for offline studies may also be utilized for voltage stability assessment of real time systems. Apart from these, new indices have also been proposed that are quite suitable in online monitoring of voltage stability margin in power system networks.

Voltage stability indices may be utilized in the current scenario in quite a large number of applications such as on-line monitoring and load shedding [4], monitoring long-term voltage stability [5], measurement of short circuit capacity [6] of the network, control of voltage when it exceeds its upper limit [7], dynamic voltage stability analysis [8], determining the proximity to collapse in real time [9], solving optimal reconfiguration problem [10], stability measurement on contingencies [11], online estimation of closeness to loadability limit [12], placement of interline power flow controller [13], improving the power system economic dispatch [14], wide area measurement based voltage stability sensitivity application in voltage control, and online voltage stability assessment [15], [16], capacitor bank allocation [17], monitoring of voltage stability margin [18], detection of cyber-attacks [19].

One of the major applications of voltage stability indices is identifying weak lines and buses that require reactive and/or real power support. That may be provided by optimally placed distributed generators (DGs). Other applications of voltage stability indices include the counter steps against voltage instability in real time framework. Online determination of voltage stability indices and counter steps against voltage instability can be obtained based on phasor measurement unit (PMU) data.

Distributed generation, often referred to as decentralized generation, embedded generation, or dispersed generation, encompasses generators with power ratings ranging from a few kilowatts to 100 megawatts. These generators are typically positioned in close proximity to the consumer's load, serving to enhance the conventional power system [20], [21]. According to the IEEE, distributed generation refers to sources that have lower ratings compared to central generation and provide sufficient flexibility to be connected at nearly any node within the network [22], [23].

Optimal placement of DGs may help in increasing voltage stability of the power system network. In this regard, numerous indices have been cited and compared vaguely in past few decades [24], [25], [26]. In [26], authors classified indices in to Jacobian matrix-based indices and system variable based indices. Also, indices have been characterized based on the basic theoretical concept, assumptions made, and condition of stability. It seems that the major research gap is the particular application of each index. The review in [25] provides background to select voltage stability indices (VSIs) for optimal DG allocation and voltage stability analysis (VSA). Voltage stability indices have also been classified based on critical lines, critical buses and system parameters such as critical eigen values, maximum loadability. A review of different voltage stability indices has been presented in [24]. However, application of these indices in monitoring health of power network has not been suggested. In [27] theoretical background, functionality and overall performance of VSIs has been discussed. But it lacks their application aspects.

While selecting VSIs for a particular application, it is worthy to understand that the indices proposed for transmission networks may not be appropriate to distribution networks. Voltage stability studies of real-time systems may be incompatible with offline study indices. Therefore, an application-oriented comparison of VSIs is presented in this article. Also, several VSIs are proposed in literature and readers find it difficult to select a particular VSI for a given application. Consequently, this article proposes a qualitative comparison for 29 VSIs which is also suited for comparing other VSIs found in the literature. Further, expanding smart grid infrastructure and increased penetration of renewable energy resources requires newer VSIs to be developed. This paper articulates some of the key challenges that need to be catered to in order to maintain voltage stability in the smart grid regime. This dossier can be utilized to comprehend the impending research in this realm and choose an apt VSI for diverse challenges in hand such as DG placing and rating, online monitoring and control of voltage stability margin, ranking the buses/lines rendering to the voltage instability, and initiating the countermeasures to curb voltage collapse.

The paper's primary objective and contributions include:

- Mathematical insight on VSIs according to the concept of the existence of solution for voltage equation, Maximum Power Transfer (MPT) through a line, MPT theorem/maximum loadability limit, P-V curve, Energy function for analysis of voltage stability, and Jacobian matrix for voltage stability analysis of the steady-state model of the power system network.
- Pointing to future research directions required to maintain voltage stability in the real-time framework and smart grid architecture.
- Proposing novel qualitative comparison of VSIs based on applications, accuracy, mode of operation, variation of VSIs with respect to system parameters, and type of stability.
- Proposing novel framework for shortlisting apt VSIs for a given problem.

In the upcoming sections, many VSIs along with their mathematical analysis has been presented in detail. The subsequent sections are organized as: Section II presents concept of power system stability along with definitions and classifications of different types of stability identified to affect power system networks. Section III provides an insight on VSIs classified on according to the concept of existence of solution for voltage equation, MPT through a line, MPT theorem/maximum loadability limit, P-V curve, Energy function for analysis of voltage stability and Jacobian matrix for voltage stability analysis of steady state model of power system network. Section IV presents comparative overview of various voltage stability indices presented in this paper. Section V specifies few research gaps and future research requirements for VSIs in growing smart grid architecture where conventional indices fail. Section VI proposes a framework for optimistically shortlisting fewer VSIs for a given problem. Finally, Section VII concludes with summary of report on listed voltage stability indices.

II. CLASSIFICATIONS OF POWER SYSTEM STABILITY

Maintaining stability in power system has been considered as an important issue since early nineteenth century. Power system stability were classified in different categories, and a report on categorization of power system stability was presented in [28]. However, due to excessive use of converter interfaced generations (CIGs), new categorization of power system stability was felt. A modified classification of power system stability has been presented in [29]. According to [25], power system stability can be described as the capacity of an electric power system to return to a state of operational equilibrium following a physical disturbance, while ensuring that the majority of system variables remain within acceptable limits, thereby preserving the overall integrity of the system. The classification of power system stability is further delineated into the subsequent categories and sub-categories.

A. VOLTAGE STABILITY

Voltage stability refers to the capacity of a power system to maintain consistent voltages in close proximity to the designated nominal value at all buses within the system subsequent to a disturbance [29]. Short-term and long-term voltage instability are caused, respectively, by the dynamics of fast- and slow-acting power system components.

B. ROTOR ANGLE STABILITY

The analysis of rotor angle stability examines the ability of interconnected synchronous machines within a power system to maintain synchronization under both normal operating conditions and when exposed to significant or minor disturbances [29]. Transient and small-disturbance rotor angle instability occur due to insufficient synchronizing and damping torque, respectively.

C. FREQUENCY STABILITY

Frequency stability refers to the capacity of the power system to sustain a consistent frequency even when exposed to a significant disparity between power generation and consumption [29]. Short-term and long-term frequency instability occur due to insufficient load shedding and improper speed control of the steam turbine, respectively.

D. RESONANCE STABILITY

The phenomenon of resonance arises when energy exchange takes place in an oscillatory manner. When the magnitude of the oscillations reaches beyond the threshold value resonance instability occurs [29]. Torsional resonance and electrical resonance occur due to the torsional frequencies of the turbine shaft and the electrical property of the generator, respectively.

E. CONVERTER DRIVEN STABILITY

The utilization of converter-interfaced generators can lead to the occurrence of cross-coupling effects, wherein the electromechanical dynamics of the generators interact with the electromagnetic transients of the power system network. The aforementioned phenomenon has the potential to result in oscillations within the power system that lack stability. Further, slow and fast interaction classification of the converter-driven stability is based on observed frequency [29].

Figure 1 shows the different classifications of the power system stability.

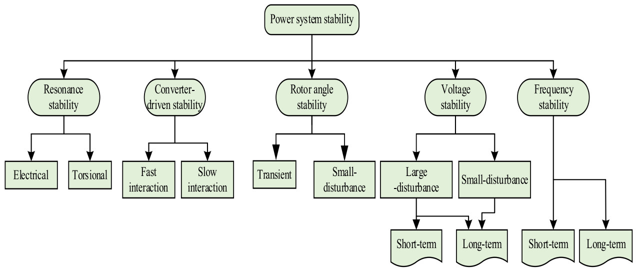

FIGURE 1. Classification of power system stability [29].

III. VOLTAGE STABILITY INDICES (VSIs)

Several VSIs have been proposed in literature based on certain assumptions that are valid in for specific networks. Some of these assumptions are valid for transmission network whereas some are valid only for distribution networks. List of assumptions along with their justification and applicability in transmission and/or distribution networks are presented in Table 1.

The properties of the voltage collapse point have been used to deduce all voltage stability indices (VSIs). Therefore, this part aims to examine these qualities in order to enhance comprehension of the Virtual Sensory Interfaces (VSIs).

A. POWER FLOW IN TWO BUS TRANSMISSION SYSTEM/ EXISTENCE OF SOLUTIONS FOR VOLTAGE EQUATION

In order to elucidate the occurrences in the area of the voltage collapse threshold, we examine the two-bus depiction of a power system network [36] as depicted in Figure 2.

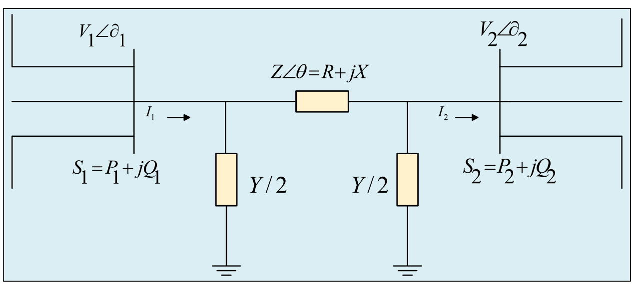

FIGURE 2. Two bus system connected through line.

The total power flow at receiving node in Figure 2 is given by eq. (1) [36]:

$$S_2 = \frac{V_1 V_2}{Z}\angle(\theta - \partial_1 + \partial_2) - \frac{V_2^2}{Z}\angle\theta \tag{1}$$

TABLE 1. Assumptions with their justifications and applicability for obtaining voltage stability indices.

S. No.	Assumptions	Justification	Applicability
A_1	Y≈0	The shunt capacitance of the line for low and medium voltages may be neglected [30].	Distribution/Transmission
A_2	P≈0	Active power may be neglected due to availability of DG-type or DG power factor [31].	Distribution/Transmission
A_3	Q≈0	Reactive power may be neglected due to availability of DG-type or DG power factor [31].	Distribution/Transmission
A_4	∂_1-∂_2≈0	Angular difference ∂_1-∂_2≈0 between typical buses of the system are usually so small [32]	Transmission system
A_5	R/X≈0	In long overhead lossless transmission line R<<X [33].	Transmission system
A_6	Π-modelled transmission line	Π-model provides better sense of physical behaviour of line. [34]	Transmission system
A_7	cosϕ constant	Power factor is assumed constant to simplify the problem. [35]	Distribution/Transmission
A_8	V_g=V_{th}	Voltage of load side generator is same as thevenin's voltage of the PSN seen from that load bus.	Transmission system
A_9	η constant	System has constant efficiency.	Transmission system
A_{10}	$N = \hat{N}$	Topological similar network after disturbance.	Transmission system
A_{11}	ΔV_2≈0, ΔI_2≈0	Voltage and current difference at receiving node is close to zero.	Transmission system
A_{12}	V_n=f(V_i)	Each node voltage is independent.	Transmission system
A_{13}	Z_{th}=0	Negligible thevenin's impedance (calculated from load side)	Transmission system
A_{14}	Whole PSN (local and remaining) is considered.		Transmission system
A_{15}	Power circles are congruent in nature.		Transmission system
A_{16}	Time interval is fixed for load bus variation.		Transmission system
A_{17}	Similar weightage is given to all lines.		Transmission system
A_{18}	Angular stability is neglected.		Transmission system
A_{19}	B≠0	Imaginary part of the line admittance is considered.	Transmission system
A_{20}	Z_L/Z_t=1	Loadability limit is independent of load power factor variation.	Distribution/Transmission
A_{21}	The bus voltage signals are normalized.		Transmission system

If $\partial = \partial_1$-∂_2, then eq. (1) can be split in to Real and Reactive power as:

$$P_2 = \frac{V_1 V_2}{Z}\cos(\theta - \partial) - \frac{V_2^2}{Z}\cos\theta \quad (2)$$

$$Q_2 = \frac{V_1 V_2}{Z}\sin(\theta - \partial) - \frac{V_2^2}{Z}\sin\theta \quad (3)$$

1) Line Stability Index (L_{mn}-index)

Solving eq. (3) for V_2 yields quadratic equation:

$$V_2^2 \sin\theta - V_1 V_2 \sin(\theta - \partial) + ZQ_2 = 0 \quad (4)$$

The condition for stability in standard quadratic equation is (i.e. $ax^2 + bx + c$): [36]

$$b^2 - 4ac \geq 0 \quad (5)$$

Thus, for eq. (4), apply condition of stability

$$[V_1 sin(\theta - \partial)]^2 - 4ZQ_2 sin\theta \geq 0 \quad (6)$$

Substituting, X= Z$\sin\theta$ in eq. (6)

$$\frac{4XQ_2}{[V_1 \sin(\theta - \partial)]^2} \leq 1 \quad (7)$$

Thus, by neglecting active power effect and shunt admittance, the Line Stability Index L_{mn} [35] can be defined as:

$$L_{mn} = \frac{4XQ_2}{[V_1 \sin(\theta - \partial)]^2} \quad (8)$$

The value of $L_{mn} = 1$, represents the stability limit.

2) Line Stability Index (L_{ij}-index)

The current in the line shown in the Figure 2 is given as:

$$I_1 = I_2 = I = \frac{V_1\angle\partial_1 - V_2\angle\partial_2}{R + jX} \quad (9)$$

Substituting,

$$\partial_1 = 0 \text{ (i.e. reference voltage angle) and } \partial_2 = \partial \quad (10)$$

The total power at receiving node is given by:

$$S_2 = V_2 I^* \quad (11)$$

$$I = \left[\frac{S_2}{V_2}\right]^* = \frac{P_2 - jQ_2}{V_2\angle - \partial} \quad (12)$$

From eq. (9) & eq. (12):

$$\frac{V_1\angle 0 - V_2\angle\partial}{R + jX} = \frac{P_2 - jQ_2}{V_2\angle - \partial} \quad (13)$$

$$V_1 V_2\angle - \partial - V_2^2\angle 0 = (R + jX)(P_2 - jQ_2) \quad (14)$$

Rearranging eq. (14):

$$V_1 V_2 \cos\partial - V_2^2 = RP_2 + XQ_2 \quad (15)$$

$$-V_1 V_2 \sin\partial = XP_2 - RQ_2 \quad (16)$$

Further, from eq. (16):

$$P_2 = \frac{RQ_2 - V_1 V_2 \sin\partial}{X} \quad (17)$$

From eq. (15) & eq. (17):

$$V_1 V_2 \cos\partial - V_2^2 = R\left\{\frac{RQ_2 - V_1 V_2 \sin\partial}{X}\right\} + XQ_2 \quad (18)$$

Rearranging the terms in eq. (18), we get:

$$V_2^2 = \left(\frac{R}{X}\sin\partial + \cos\partial\right) V_1 V_2 + \left(X + \frac{R^2}{X}\right) Q_2 = 0 \quad (19)$$

Applying the condition of stability on eq. (19):

$$\left[\left(\frac{R}{X}\sin\partial + \cos\partial\right) V_1\right]^2 - 4\left(X + \frac{R^2}{X}\right) Q_2 \geq 0 \quad (20)$$

or

$$\frac{4Z^2 Q_2 X}{V_1^2(R\sin\partial + X\sin\partial)^2} \leq 1 \quad (21)$$

Thus, by neglecting shunt admittance an index can be derived as [37]

$$L_{ij} = \frac{4Z^2 Q_2 X}{V_1^2(R\sin\partial + X\cos\partial)^2} \quad (22)$$

3) Fast Voltage Stability Index (FVSI)

Further taking assumptions $\sin\partial \approx 0$, $\cos\partial \approx 1$, $R\sin\partial \approx 0$, $X\cos\partial \approx X$ in eq. (22), the FVSI [38] is obtained as:

$$FVSI = \frac{4Z^2 Q_2}{V_1^2 X} \quad (23)$$

The FVSI and L_{ij} should be less than 1 for stable operation of power system.

4) NEW VOLTAGE STABILITY INDEX (NVSI)

On solving eq. (15) and eq. (16) for P_2 and Q_2:

$$P_2 = [(V_1 cos\partial - V_2)\frac{R}{(R^2 + X^2)} - (V_1 sin\partial)\frac{X}{(R^2 + X^2)}]V_2 \quad (24)$$

$$Q_2 = [(V_1 cos\partial - V_2)\frac{X}{(R^2 + X^2)} - (V_1 sin\partial)\frac{R}{(R^2 + X^2)}]V_2 \quad (25)$$

For lossless line R/X≪1, Thus:

$$P_2 = \frac{V_1 V_2 \sin\partial}{X} \quad (26)$$

$$Q_2 = \frac{V_1 V_2 \cos\partial - V_2^2}{X} \quad (27)$$

Applying $\cos^2\theta + \sin^2\theta = 1$ on eq. (26) & eq. (27):

$$V_2^4 + (2Q_2 X - V_1^2)V_2^2 + Q_2^2 X^2 + P_2^2 X^2 = 0 \quad (28)$$

Further, applying stability criterion on eq. (28):

$$\left[(2Q_2 X - V_1^2)\right]^2 - 4\left(Q_2^2 X^2 + P_2^2 X^2\right) \geq 0 \quad (29)$$

$$\frac{2X\sqrt{P_2^2 + Q_2^2}}{2Q_2 X - V_1^2} \leq 1 \quad (30)$$

Thus, by assuming lossless line, NVSI [39] can be defined as:

$$NVSI = \frac{2X\sqrt{P_2^2 + Q_2^2}}{2Q_2X - V_1^2} \tag{31}$$

For the stable operation NVSI should be less than 1.

5) LINE STABILITY FACTOR (LQP)

On expanding eq. (29):

$$V_1^4 + 4Q_2XV_1^2 + 4P_1^2X^2 \geq 0 \tag{32}$$

$$1 + \frac{4Q_2X}{V_1^2} + \frac{4P_1^2X^2}{V_1^4} \geq 0 \tag{33}$$

$$4\left[\frac{X}{V_1^2}\right]\left[\frac{X}{V_1^2}P_1^2 + Q_2\right] \leq 1 \tag{34}$$

Further, assuming lossless line (i.e. R/X≪1), LQP [40] can be defined as:

$$LQP = 4\left[\frac{X}{V_1^2}\right]\left[\frac{X}{V_1^2}P_1^2 + Q_2\right] \tag{35}$$

For the stability, line stability factor (i.e. LQP) must be less than 1.

6) LINE STABILITY INDEX (L_P-INDEX)

Solving eq. (2) for V_2 yields:

$$V_2^2\cos\theta - V_1V_2\cos(\theta - \partial) + ZP_2 = 0 \tag{36}$$

Applying condition for stability on eq. (36).

$$[V_1\cos(\theta - \partial)]^2 - 4ZP_2\cos\theta \geq 0 \tag{37}$$

Substituting, R= Zcosθ in eq. (35)

$$V_1^2\cos^2(\theta - \partial) - 4RP_2 \geq 0 \tag{38}$$

$$\frac{4RP_2}{V_1^2\cos^2(\theta - \partial)} \leq 1 \tag{39}$$

Thus, by neglecting the effect of shunt admittance and reactive power, L_p [41] can be given as

$$L_P = \frac{4RP_2}{V_1^2\cos^2(\theta - \partial)} \tag{40}$$

Line stability index L_p is designed in such a manner that if its value is more than 1, system will be unstable.

7) NEW LINE STABILITY INDEX (NLSI)

From eq. (15),

$$V_2^2 - V_1V_2\cos\partial + RP_2 + XQ_2 = 0 \tag{41}$$

Applying the condition of stability on eq. (41),

$$[V_1\cos\partial]^2 - 4\left(RP_2 + XQ_2\right) \geq 0 \tag{42}$$

$$\frac{RP_2 + XQ_2}{0.25V_1^2\cos^2\partial} \leq 1 \tag{43}$$

Thus, by neglecting shunt admittance and angle difference between both end voltages, NLSI [42] can be defined as:

$$NLSI = \frac{RP_2 + XQ_2}{0.25V_1^2} \tag{44}$$

The value for stability limit of NLSI is 1 i.e. if NLSI>1, system becomes unstable.

8) VOLTAGE REACTIVE POWER INDEX (VQI_{Line})

From eq. (9) and (12) apparent power is given as:

$$S = P_2 - jQ_2 = V_1V_2Y_{12}\angle(\theta - \partial) - V_2^2Y_{12}\angle\theta \tag{45}$$

Hence, real and reactive power are given as:

$$P_2 = V_1V_2Y_{12}\cos(\theta - \partial) - V_2^2Y_{12}\cos\theta \tag{46}$$

$$Q_2 = V_1V_2Y_{12}\sin(\theta - \partial) - V_2^2Y_{12}\sin\theta \tag{47}$$

Rearranging the eq. (47) as a quadratic equation in term of V_2 as:

$$V_2^2 - V_1V_2\frac{\sin(\theta - \partial)}{\sin\theta} + \frac{Q_2}{Y_{12}\sin\theta} = 0 \tag{48}$$

Neglecting voltage angle difference of both ends, the term sin(θ-∂)/sinθ is eliminated and thus:

$$V_2^2 - V_1V_2 + \frac{Q_2}{Y_{12}\sin\theta} = 0 \tag{49}$$

Substituting $B_{12} = Y_{12}\sin\theta$, eq. (49) can be rewritten as

$$V_2^2 - V_1V_2 + \frac{Q_2}{B_{12}} = 0 \tag{50}$$

Applying the condition of stability on eq. (50), we get

$$V_1^2 - 4\frac{Q_2}{B_{12}} \geq 0 \tag{51}$$

Hence, for stability:

$$\frac{4Q_2}{B_{12}V_1^2} \leq 1 \tag{52}$$

Thus, VQI_{Line} [43] is given as:

$$VQI_{Line} = \frac{4Q_2}{B_{12}V_1^2} \tag{53}$$

The critical value of VQI_{Line} for voltage collapse is 1.

9) VOLTAGE STABILITY LOAD INDEX (VSLI)

From eq. (12),

$$I_2^2 = \frac{P_2^2 + Q_2^2}{V_2^2} \tag{54}$$

$$I_1^2 = \frac{P_1^2 + Q_1^2}{V_1^2} \tag{55}$$

$$P_2 = P_1 - P_{loss} \tag{56}$$

$$Q_2 = Q_1 - Q_{loss} \tag{57}$$

$$P_{loss} = \left(\frac{P_2^2 + Q_2^2}{V_2^2}\right)^2 R \tag{58}$$

$$Q_{loss} = \left(\frac{P_2^2 + Q_2^2}{V_2^2}\right)^2 X \tag{59}$$

Substituting eq. (56)-(59) in eq. (55), we obtain:

$$I_1^2 = \frac{\left[P_2 + \left(\frac{P_2^2+Q_2^2}{V_2^2}\right) R\right]^2}{V_1^2} + \frac{\left[Q_2 + \left(\frac{P_2^2+Q_2^2}{V_2^2}\right) X\right]^2}{V_1^2} \tag{60}$$

From eq. (9) $I_1 = I_2$ and combining eq. (54) and eq. (60) lead to

$$V_1^2 = V_2^2 + 2\left(P_2R + Q_2X\right) + \left(\frac{P_2^2 + Q_2^2}{V_2^2}\right)\left(R^2 + X^2\right) \tag{61}$$

From eq. (61), the voltage equation could be written as:

$$V_2^4 + V_2^2\left[2\left(P_2R + Q_2X\right) - V_1^2\right] + \left(P_2^2 + Q_2^2\right)\left(R^2 + X^2\right) = 0 \tag{62}$$

Applying the condition of stability on eq. (62), we get

$$\frac{4\left[V_1^2\left(P_2R + Q_2X\right) + \left(P_2R + Q_2X\right)^2\right]}{V_1^4} \leq 1 \tag{63}$$

Therefore, the VSLI [44], [45] is given as

$$VSLI = \frac{4\left[V_1^2\left(P_2R + Q_2X\right) + \left(P_2R + Q_2X\right)^2\right]}{V_1^4} \tag{64}$$

VSLI must be less than 1 for the stability. VSLI can be calculated with the help of Phasor Measurement Unit (PMU) data.

10) VOLTAGE STABILITY INDEX (L-INDEX)

From eq. (15) & (16):

$$V_1V_2\cos\partial - V_2^2 = P_2R + Q_2X \tag{65}$$

$$-V_1V_2\sin\partial = P_2X - Q_2R \tag{66}$$

Substituting the eq. (65) and (66) in (64):

$$VSLI = \frac{4\left[V_1V_2\cos\partial - V_2^2\cos^2\partial\right]}{V_1^2} \tag{67}$$

By neglecting the voltage angle difference, voltage stability index L [46] may be deduced as:

$$L = \frac{4\left[V_1V_2 - V_2^2\right]}{V_1^2} \tag{68}$$

The condition for stability is same as that of VSLI.

11) VOLTAGE STABILITY INDICATOR (VSI_B)

Equation (14) after neglecting the voltage angle difference:

$$V_1V_2 - V_2^2 = (R + jX)(P_2 - jQ_2) \tag{69}$$

Further rearranging the terms in eq. (69):

$$V_1V_2 - V_2^2 = (RP_2 + XQ_2) + j(XP_2 - RQ_2) \tag{70}$$

On comparing real part:

$$V_1V_2 - V_2^2 = RP_2 + XQ_2 \tag{71}$$

Rearranging:

$$\frac{R}{X}V_2^2 - \frac{R}{X}V_1V_2 + \left[P_2\left(\frac{R^2}{X} - X\right) + 2RQ_2\right] = 0 \tag{72}$$

Applying the condition of stability on eq. (72),

$$\frac{4Q\left(R + X\right)^2}{X\left(V_1^2 + 8RQ_2\right)} \leq 1 \tag{73}$$

Hence, VSI_B [47] is represented by

$$VSI_B = \frac{4Q_2\left(R + X\right)^2}{X\left(V_1^2 + 8RQ_2\right)} \tag{74}$$

The stability limit of VSI_B is 1.

12) STABILITY INDEX (SI)

From eq. (62),

$$P_2 = \left[\begin{array}{l} -V_2^2\cos\theta \pm \sqrt{(V_2^4\cos^2\theta - V_2^4} \\ -|Z|^2 Q_2^2 - 2V_2^2Q_2X + V_1^2V_2^2) \end{array}\right] / |Z| \tag{75}$$

$$Q_2 = \left[\begin{array}{l} -V_2^2\sin\theta \pm \sqrt{(V_2^4\sin^2\theta - V_2^4} \\ -|Z|^2 P_2^2 - 2V_2^2P_2R + V_1^2V_2^2) \end{array}\right] / |Z| \tag{76}$$

From eq. (75) & (76) for the real values of P_2 & Q_2, following conditions must be satisfied,

$$V_2^4\cos^2\theta - V_2^4 - |Z|^2 Q^2 - 2V_2^2QX + V_1^2V_2^2 \geq 0 \tag{77}$$

$$V_2^4\sin^2\theta - V_2^4 - |Z|^2 P^2 - 2V_2^2PR + V_1^2V_2^2 \geq 0 \tag{78}$$

Summing eq. (77) & (78),

$$2V_1^2V_2^2 - V_2^4 - 2V_2^2\left(P_2R + Q_2X\right) - |Z|^2\left(P_2^2 + Q_2^2\right) \geq 0 \tag{79}$$

Thus, the SI [48] can be written as

$$SI = 2V_1^2V_2^2 - V_2^4 - 2V_2^2\left(P_2R + Q_2X\right) - |Z|^2\left(P_2^2 + Q_2^2\right) \tag{80}$$

The stability index derived above is based on voltage quadratic equation. The critical value of SI is 0, beyond which system becomes unstable.

13) LINE COLLAPSE PROXIMITY INDEX (LCPI)

Transmission line may be modelled with the help of two port equivalent network as:

$$\begin{pmatrix} V_1 \\ I_1 \end{pmatrix} = \begin{pmatrix} A & B \\ C & D \end{pmatrix} \begin{pmatrix} V_2 \\ I_2 \end{pmatrix} \tag{81}$$

$$V_1\angle\partial_1 = A\angle\alpha V_2\angle\partial_2 + B\angle\beta I_2\angle 0 \tag{82}$$

Putting the value of current I_2 from eq. (12),

$$V_1\angle\partial_1 = A\angle\alpha V_2\angle\partial_2 + B\angle\beta \left(\frac{P_2 - jQ_2}{V_2\angle - \partial_2}\right) \tag{83}$$

Rearranging eq. (83), yields

$$V_1 V_2\angle\left(\partial_1 - \partial_2\right) = A\angle\alpha V_2^2 + B\angle\beta \left(P_2 - jQ_2\right) \tag{84}$$

Replacing ∂_1-∂_2 by ∂ and rearranging eq. (84),

$$V_2^2 \left(A\cos\alpha\right) - V_2\left(V_1\cos\partial\right) + \left(P_2 B\cos\beta + Q_2 B\sin\beta\right) = 0 \tag{85}$$

Applying the condition of stability on eq. (85):

$$\left(V_1\cos\partial\right)^2 - 4\left(A\cos\alpha\right)\left(P_2 B\cos\beta + Q_2 B\sin\beta\right) \geq 0 \tag{86}$$

or

$$\frac{4\left(A\cos\alpha\right)\left(P_2 B\cos\beta + Q_2 B\sin\beta\right)}{\left(V_1\cos\partial\right)^2} \leq 1 \tag{87}$$

Thus, LCPI [49] may be defined as

$$LCPI = \frac{4\left(A\cos\alpha\right)\left(P_2 B\cos\beta + Q_2 B\sin\beta\right)}{\left(V_1\cos\partial\right)^2} \tag{88}$$

The stability limit for LCPI is 1.

B. MPT / MAXIMUM POWER LOSS THROUGH A LINE

A power system network may be represented as two bus Thevenin's equivalent system as shown in Figure 3.

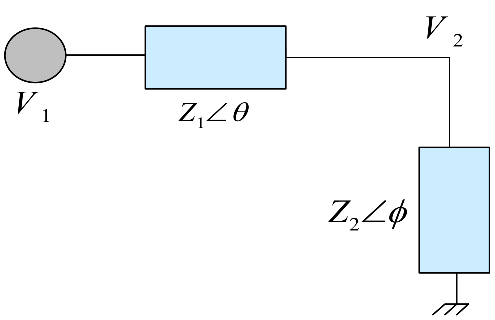

FIGURE 3. Representation of power system network through Thevenin's equivalent network [50].

The current I flowing through the Thevenin's equivalent circuit is:

$$I = \frac{V_1}{\sqrt{\left[\left(Z_1\cos\theta + Z_2\cos\phi\right)^2 + \left(Z_1\sin\theta + Z_2\sin\phi\right)^2\right]}}$$

$$= \frac{I_{cc}}{\sqrt{\left[1 + \left(Z_2/Z_1\right)^2 + 2\left(Z_2/Z_1\right)\cos\left(\theta - \phi\right)\right]}} \tag{89}$$

$$V_2 = Z_2 I = \frac{Z_2 I_{cc}}{\sqrt{\left[1 + \left(Z_2/Z_1\right)^2 + 2\left(Z_2/Z_1\right)\cos\left(\theta - \phi\right)\right]}} \tag{90}$$

where short circuit current, $I_{cc} = V_1/Z_1$.

$$P_2 = V_2 I\cos\phi = Z_2 I^2\cos\phi$$

$$P_2 = \frac{Z_2 I_{cc}^2}{\left[1 + \left(Z_2/Z_1\right)^2 + 2\left(Z_2/Z_1\right)\cos\left(\theta - \phi\right)\right]}\cos\phi \tag{91}$$

For MPT, $\partial P_2/\partial Z_2 = 0$, thus:

$$Z_2/Z_1 = 1 \tag{92}$$

Similarly,

$$Q_2 = \frac{Z_2 I_{cc}^2}{\left[1 + \left(Z_2/Z_1\right)^2 + 2\left(Z_2/Z_1\right)\cos\left(\theta - \phi\right)\right]}\sin\phi \tag{93}$$

The wattage loss through line is given by $P_l = I_2 Z_1\cos\theta$ and $Q_l = I_2 Z_1\sin\theta$. Which can further be written as:

$$P_l = \frac{\left(V_1\right)^2/Z_1}{1 + \left(Z_2/Z_1\right)^2 + 2\left(Z_2/Z_1\right)\cos\left(\theta - \phi\right)}\cos\theta \tag{94}$$

and

$$Q_l = \frac{\left(V_1\right)^2/Z_1}{1 + \left(Z_2/Z_1\right)^2 + 2\left(Z_2/Z_1\right)\cos\left(\theta - \phi\right)}\sin\theta \tag{95}$$

1) GENERALIZATION TO AN ACTUAL NETWORK

Thevenin's theorem states that any linear network with energy source can be shown by a network consisting of a voltage source (V_{th}) in series with equivalent impedance (Z_{th}) [50]. Thus, for a n-bus power system network if the Thevenin's equivalent impedance is $Z_{ii}\angle\theta_i$ and load impedance is $Z_i\angle\Phi_i$, power will be transferred to load when $Z_{ii}/Z_i \leq 1$.

2) LINEARIZED MODEL FOR POWER SYSTEM NETWORK

Nonlinearities in the PSN is caused by the presence of nonlinear elements (i.e. generators, loads etc.), however, Thevenin's theorem is applicable to linear system only. Therefore, system is linearized at operating point as:

$$Z_2\angle\phi_2 = \frac{V_2}{I_2}\angle\phi_2 = \frac{V_2^2\cos\phi_2}{V_2 I_2\cos\phi_2}\angle\phi_2 = \frac{V_2^2\cos\phi_2}{P_2}\angle\phi_2$$

where,

$$\angle\phi_2 = \tan^{-1}\left(Q_2/P_2\right)$$

Let, Z_1 = source feeder internal impedance, and Z_2 = load feeder impedance in Figure 3. Determination of Thevenin's impedance and no-load voltage are discussed in detail by [50].

3) VOLTAGE COLLAPSE PROXIMITY INDICATORS (VCPI)

Maximum power transfer (MPT) at receiving end is:

$$P_{2(\max)} = \frac{V_1^2}{Z_1} \times \frac{\cos\phi}{4\cos^2\frac{(\theta-\phi)}{2}} \tag{96}$$

and,

$$Q_{2(\max)} = \frac{V_1^2}{Z_1}\frac{\sin\phi}{4\cos^2\frac{(\theta-\phi)}{2}} \tag{97}$$

Similarly,

$$P_{l(\max)} = \frac{V_1^2}{Z_1}\frac{\cos\theta}{4\cos^2\frac{(\theta-\phi)}{2}} \tag{98}$$

and,

$$Q_{l(\max)} = \frac{V_1^2}{Z_1}\frac{\sin\theta}{4\cos^2\frac{(\theta-\phi)}{2}} \tag{99}$$

These are the maximum permissible quantities. On the basis of these maximum permissible quantities, the following VCPI [35] are given:

$$VCPI\ (1) = \frac{P_2}{P_{2(\max)}} \tag{100}$$

$$VCPI\ (2) = \frac{Q_2}{Q_{2(\max)}} \tag{101}$$

$$VCPI\ (3) = \frac{P_l}{P_{l(\max)}} \tag{102}$$

$$VCPI\ (4) = \frac{Q_l}{Q_{l(\max)}} \tag{103}$$

For the ease of identification, all VCPIs are represented as VCPI $_{(\text{power})}$ and VCPI $_{(\text{loss})}$. As the loading at the receiving end reaches to critical value both indices approach to 1. It is observed that close to voltage collapse point VCPI $_{(\text{power})}$ is less sensitive as compared to VCPI $_{(\text{loss})}$ for further loading [35].

4) NEW VOLTAGE STABILITY INDEX (L_{sr})

The total power flow in Figure 3 is given by

$$S_2 = V_2 I \tag{104}$$

From eq. (89) and eq. (90)

$$S_2 = \frac{V_1^2}{Z_1}\frac{1}{\left[1+(Z_2/Z_1)^2+2\,(Z_2/Z_1)\cos(\theta-\phi)\right]}\frac{Z_2}{Z_1} \tag{105}$$

and the MPT is given by:

$$S_{2(\max)} = \frac{V_1^2}{4Z_1}\frac{1}{\cos^2\left(\frac{\theta-\phi}{2}\right)} \tag{106}$$

On the basis of previous assumptions the new VSI, L_{sr} [51] is given as:

$$L_{sr} = \frac{S_2}{S_{2(\max)}} \tag{107}$$

5) POWER SYSTEM STABILITY INDEX (PTSI)

Current through the load in the Figure 3 is given as:

$$I = \frac{V_1}{Z_1\angle\theta + Z_2\angle\phi} \tag{108}$$

Apparent power at load side is give as:

$$S_2 = Z_2\angle\phi\,|I|^2 = \frac{V_1^2 Z_2}{|Z_1\angle\theta + Z_2\angle\phi|^2} = \frac{V_1^2 Z_2}{Z_1^2+Z_2^2+2Z_1Z_2\cos(\theta-\phi)} \tag{109}$$

where $V_1, Z_1, \& Z_2$ may be considered as Thevenin's voltage, Thevenin's impedance and Load impedance, respectively.

Maximum power through the load may be given as:

$$S_{2(\max)} = \frac{V_1^2}{2Z_1\,(1+\cos(\theta-\phi))} \tag{110}$$

The voltage collapse occurs if the ratio $S_2/S_{2(\max)} = 1$.

With the help of eq. (109), (110) and neglecting shunt admittance, the PTSI [52] can be given as:

$$PTSI = \frac{2S_2Z_1\,(1+\cos(\theta-\phi))}{V_1^2} \tag{111}$$

The maximum value of PTSI for stability is 1.

6) VOLTAGE STABILITY INDEX (VSI)

Combining eq. (24) & eq. (25) with the assumption of ∂ being negligible

$$V_2 = \sqrt{\frac{V_1^2}{2} - (QX+PR) \pm \sqrt{A}} \tag{112}$$

where,

$$A = \frac{V_1^2}{4} - (QX+PR)\,V_1^2 - (PX-QR)^2 \tag{113}$$

Therefore, for the real solution of eq. (112), A must not be negative. Hence,

$$A \geq 0 \tag{114}$$

From eq. (24) and eq. (25), maximum Real power demand P_2(max), maximum VAr power demand $Q_{2(\max)}$ and maximum VA power demand $S_{2(\max)}$ can be calculated by assuming VAr power demand Q_2, Real power demand P_2 and load power factor angle, Φ, constant.

$$P_{2(\max)} = \frac{Q_2R}{X} - \frac{V_1^2R}{2X^2} + \frac{|Z_2|\,V_1\sqrt{V_1^2-4Q_2X}}{2X^2} \tag{115}$$

$$Q_{2(\max)} = \frac{P_2X}{R} - \frac{V_1^2X}{2R^2} + \frac{|Z_2|\,V_1\sqrt{V_1^2-4P_2R}}{2R^2} \tag{116}$$

$$S_{2(\max)} = \frac{V_1^2\left[|Z_2| - (\sin(\phi)\,X + \cos(\phi)\,R)\right]}{2\,(\cos(\phi)\,X - \sin(\phi)\,R)^2} \tag{117}$$

Since for transmission line X/R≫1, the approximate value of $P_{2(max)}$, $Q_{2(max)}$ and $S_{2(max)}$ can be expressed as:

$$P_{2(max)} = \sqrt{\frac{V_1^4}{4X^2} - Q_2\frac{V_1^2}{X}} \tag{118}$$

$$Q_{2(\max)} = \frac{V_1^2}{4X} - \frac{P_2^2 X}{V_1^2} \tag{119}$$

$$S_{2(\max)} = \frac{(1-\sin(\phi))\,V_1^2}{2\cos^2(\phi)\,X} \tag{120}$$

With the approximate $P_{2(max)}$, $Q_{2(max)}$ and $S_{2(max)}$ three load margins P_{margin}, Q_{margin} and S_{margin} is calculated as:

$$P_{m\arg in} = P_{2(\max)} - P_2 \tag{121}$$

$$Q_{m\arg in} = Q_{2(\max)} - Q_2 \tag{122}$$

$$S_{m\arg in} = S_{2(\max)} - S_2 \tag{123}$$

The derived VSI [53] based on the load margins can be written as

$$VSI = \min\left(\frac{P_{m\arg in}}{P_{2(\max)}}, \frac{Q_{m\arg in}}{Q_{2(\max)}}, \frac{S_{m\arg in}}{S_{2(\max)}}\right) \tag{124}$$

Lower values of VSI indicates marginal stable point.

7) VOLTAGE STABILITY MARGIN (VSM_S)

From the eq. (90), the voltage across the load impedance Z_2 is given as:

$$V_2 = \frac{V_1 Z_2}{\sqrt{[Z_2^2 + Z_1^2 + 2Z_1Z_2\cos(\theta-\phi)]}} \tag{125}$$

$$S_2 = V_2^2 \Big/ Z_2 = \frac{V_2^2 Z_2}{[Z_2^2 + Z_1^2 + 2Z_1Z_2\cos(\theta-\phi)]} \tag{126}$$

The power at critical point is given as:

$$S_{cr} = \frac{V_2^2}{2Z_1\,[1+\cos[\theta-\phi]]} \tag{127}$$

Z_2-Z_1 may be considered as margin of safety for given Z_2. On the basis of this VSM in terms of impedance VSM_z may be defined as:

$$VSM_z = \frac{Z_2 - Z_1}{Z_1} \tag{128}$$

Further, VSM in terms of power VSM_s [54] is represented as:

$$VSM_s = \frac{S_{cr} - S_2}{S_{cr}} \tag{129}$$

For stability point of view VSM_s must be greater than zero.

8) VOLTAGE STABILITY MARGIN INDEX (VSMI)

The equations of Watt and VAr power flow in Figure 3 [32] is given by:

$$V_2 = V_1\frac{\cos(\phi+\partial)}{\cos\phi} \tag{130}$$

$$P_2 = \frac{1}{2}\frac{V_1^2}{X}\left(\frac{\sin(\phi+2\partial)}{\cos\phi} - \tan\phi\right) \tag{131}$$

where, $\tan(\phi) = \frac{Q_2}{P_2}$. The maximum value of P_2 and V_2 can be found from the eq. (130) and eq. (131) for any given value of Φ as:

$$P_{2(\max)} = \frac{1}{2}\frac{V_1^2}{X}\left(\frac{1}{\cos\phi} - \tan\phi\right) \tag{132}$$

$$V_{2(\max)} = \frac{\cos\left(\frac{\pi}{2}+\phi\right)}{\cos\phi}V_1 \tag{133}$$

when,

$$\partial_{\max} = \frac{\frac{\pi}{2}-\phi}{2} \tag{134}$$

As the ∂ reaches to ∂_{max}, corresponding values of $P_{2(max)}$ and $V_{2(max)}$ can be calculated from knee point of PV curve [55]. Hence the VSM can be the angular distance between ∂ & ∂_{max}. As said earlier, for any given working condition of load the VSMI [51] is:

$$VSMI = \frac{\partial_{\max} - \partial}{\partial_{\max}} \tag{135}$$

C. MPT THEOREM

Any intricate power system network may be reduced to the equivalent Thevenin's network with Thevenin's voltage V_1 and Thevenin's impedance Z_1 [56]. The load voltage V_2 and load side apparent power S_2 is given in eq. (125) and eq. (126).

Apparent power sensitivity for load admittance is given as:

$$\frac{dS_2}{dY_2} = \frac{V_2\left[1-(Z_1Y_2)^2\right]}{1+(Z_1Y_2)^2+2Z_1Y_2\cos\partial} \tag{136}$$

where $Y_2 = 1/Z_2$

Dividing both side by $(V_2)^2$

$$\frac{dS_2^*}{dY_2^*} = \frac{1-(Z_1Y_2)^2}{1+(Z_1Y_2)^2+2Z_1Y_2\cos\partial} \tag{137}$$

Substituting, $dS_2/dY_2 = (Y_2/S_2)\, dS_2/dY_2$ in eq. (136)

$$\frac{Z_2}{Z_1} = \frac{M+1}{-M\cos\partial + \sqrt{[(M\cos\partial)^2 - M^2 + 1]}} \tag{138}$$

where, $M = dS_2^*/dY_2^* = (S_3\text{-}S_1)(Y_2+Y_1)/(S_2+S_1)(Y_2\text{-}Y_1)$, S_1, Y_1 are complex power drawn by the load and admittance at the beginning (t_1), S_2, Y_2 are load power and admittance at the end (t_2). For stable operation, the ratio $Z_2/Z_1 \geq 1$ [57]. This ratio is also used to initiate load shedding under critical situation of the system.

1) SIMPLIFIED VOLTAGE STABILITY INDEX (SVSI)

The concept of SVSI is based on relative electric distance (RED). The concept RED is to find generator node near to the load node to enhance its performance. In matrix form the generator & load node currents can be related to the respective node voltages as

$$\begin{bmatrix} I_G \\ I_L \end{bmatrix} = \begin{bmatrix} Y_{GG} & Y_{GL} \\ Y_{LG} & Y_{LL} \end{bmatrix}\begin{bmatrix} V_G \\ V_L \end{bmatrix} \tag{139}$$

Rearranging the matrix eq. (139)

$$\begin{bmatrix} V_L \\ I_G \end{bmatrix} = \begin{bmatrix} Z_{LL} & F_{LG} \\ K_{GL} & Y_{GG} \end{bmatrix} \begin{bmatrix} I_L \\ V_G \end{bmatrix} \tag{140}$$

where, $F_{LG} = -|Y_{LL}|^{-1}|Y_{LG}|$ [58].

$$R_{LG} = [A] - abs\,[F_{LG}] = [A] - abs\left(|Y_{LL}|^{-1}|Y_{LG}|\right) \tag{141}$$

where, [A] is unit matrix of dimension (n-g)×(g).

The voltage drop ΔV_i on the Thevenin's impedance can be calculated as

$$\Delta V_i = \sum_{b=1}^{n_j-1}\left|\vec{V_b} - \overrightarrow{V_{b+1}}\right| \cong \left|\vec{V_g} - \vec{V_i}\right| \tag{142}$$

The above eq. (142) is the useful simplification of the originally proposed method in [59]. A correction factor β is proposed in [60] to increase the sensitivity of the derived index and excel its performance. The correction factor β is given by:

$$\beta = 1 - (\max(|V_m| - |V_l|))^2 \tag{143}$$

The difference of voltage magnitude ($|V_m|$ - $|V_i|$) of two buses is found out from PMU measurement [60]. The SVSI for the i^{th} bus is defined as:

$$SVSI = \frac{\Delta V_i}{\beta V_i} \tag{144}$$

Power system network will be voltage stable when the proposed index is greater than unity.

Local VSI [61] is obtained from the concept of Tellegen's theorem (TT) and adjoint networks. In this method, Telligen's Theorem is used to derive Thevenin's parameters. The basic form of Telligen's Theorem states that:

$$V^T I = 0 \tag{145}$$

The Telligen's Theorem may be expressed in another form as,

$$\hat{I}^T \Delta V - \hat{V}^T \Delta I = 0 \tag{146}$$

where,

ΔV: voltage of incremented network
ΔI: current of incremented network
$\hat{I}$: current of adjoint network
$\hat{V}$: voltage of adjoint network

Equation (146) is valid only if the base network and adjoint network are topologically identical. Adjoint networks are unaffected by above mentioned disturbances because it is physically decoupled from the base network.

We may categorize ΔV, ΔI, and into three groups slack bus, remaining buses & network branches.

Now the eq. (146) may be rewritten as:

$$\left(\hat{I}_S^T \Delta V_S - \hat{V}_S^T \Delta I_S\right) + \left(\hat{I}_P^T \Delta V_P - \hat{V}_P^T \Delta I_P\right) + \left(\hat{I}_B^T \Delta V_B - \hat{V}_B^T \Delta I_B\right) = 0 \tag{147}$$

Since reference bus has no contribution in eq. (147). Thus

$$\left(\hat{I}_S^T \Delta V_S - \hat{V}_S^T \Delta I_S\right) = 0 \tag{148}$$

Without changing the topology of adjoint network eq. (148) can be further developed to depict the voltage sensitivities of system component for power & network disturbances.

$$\left(\hat{I}_B^T \Delta V_B - \hat{V}_B^T \Delta I_B\right) = 0 \tag{149}$$

Hence,

$$\left(\hat{I}_P^T \Delta V_P - \hat{V}_P^T \Delta I_P\right) = 0 \tag{150}$$

Taking complex conjugate [61] of eq. (150)

$$\left(\hat{I}_P^* \Delta V_P - \hat{V}_P^T \Delta I_P^*\right) = 0 \tag{151}$$

or

$$\left(\hat{I}_P^T \Delta V^*{}_P - \hat{V}^*{}_P^T \Delta I_P\right) = 0 \tag{152}$$

Thevenin's equivalent network N, and the corresponding adjoint network $\hat{N}$ of a power system supplying load connected at bus-k (Figure 4(a)) are shown in Figure 4(b) and Figure 4(c), respectively.

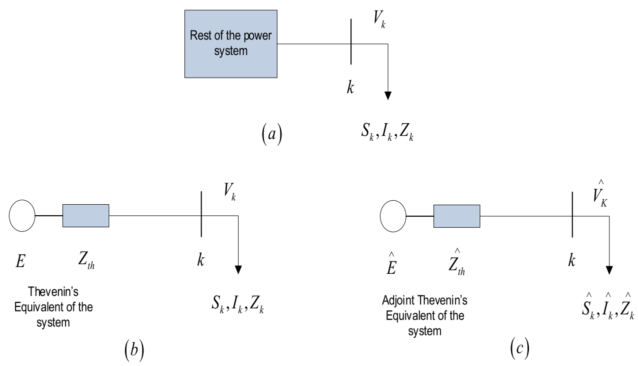

FIGURE 4. (a) General representation of load bus k in a power system, (b) the corresponding network N, and (c) its adjoint network $\hat{N}$.

2) IMPEDANCE-STABILITY INDEX (ISI)

The current in Figure 4(b) will be

$$S_k/V_k = I_k^* = \left((E - V_k)/Z_{th}\right) \tag{153}$$

or

$$V_k (E - V_k)^* - S_k Z_{th}^* = 0 \tag{154}$$

Maximum power is transferred when

$$V_k = (E - V_k)^* \tag{155}$$

On the basis of stability criterion, eq. (155) facilitates following result of circuit theory.

$$|Z_k| = |Z_{th}| \tag{156}$$

Equation (156) shows the condition for maximum power transfer. The maximum power transfer (MPT) is a limit towards loading. Beyond this limit, equilibrium will be lost and voltage collapse occurs [62]. Hence, eq. (156) denotes stability limit.

Similarly, for adjoint network eq. (153)-(156) can also be rewritten with cap (∧)z. The eq. (146) can be rewritten for kth bus as

$$\left(\hat{I}^{*T}_{k}\Delta V_k - \hat{V}_k^T\Delta I_k^*\right) = 0 \tag{157}$$

On the basis of real time measurement of voltage & current difference, the impedance for kth bus is given as:

$$\hat{Z}_k = \left|\hat{Z}_k\right| = \left|\hat{V}_k/\hat{I}_k\right| \tag{158}$$

From eq. (157) and eq. (158) adjoint Thevenin's impedance can be derived as:

$$\left(\left(\hat{E} - \hat{V}_k\right)/\hat{Z}_{th}\right)^* \Delta V_k - \hat{V}_k\Delta I_k^* = 0 \tag{159}$$

$$\hat{Z}_{th}^* = \left(\left(\hat{E} - \hat{V}_k\right)^* / \left(\hat{V}_k\Delta I_k^*\right)\right)\Delta V_k \tag{160}$$

MPT in adjoint network occurs when

$$\hat{V}_k = (\hat{E} - \hat{V})^* \tag{161}$$

Comparing eq. (160) & (161), the Thevenin's impedance at the voltage collapse point is as follows:

$$\hat{Z}_{th}^* = \Delta V_k/\Delta I_k{}^* \tag{162}$$

or

$$\hat{Z}_{th} = \Delta V_k^*/\Delta I_k \tag{163}$$

or

$$\hat{Z}_{th} = \left|\hat{Z}_{th}\right| = |\Delta V_k/\Delta I_k| \tag{164}$$

At base load:

$$\hat{Z}_k \gg \hat{Z}_{th} \tag{165}$$

At the voltage collapse point, $\hat{Z}_k = \hat{Z}_{th}$

$$\hat{Z}_k = \hat{Z}_{th}\left|\Delta V_k/\Delta I_k\right| = \left|V_k/I_k\right| \tag{166}$$

Considering eq. (165) and eq. (166), a impedance-stability index (ISI) [61] for determining the voltage stability margin (VSM) can be defined as:

$$ISI = \frac{\left(\hat{Z}_k - \hat{Z}_{th}\right)}{\hat{Z}_k} \tag{167}$$

or

$$ISI = 1 - |I_k\Delta V_k|\big/|V_k\Delta I_k| \tag{168}$$

3) VOLTAGE STABILITY INDEX (VSI$_{bus}$)

Equation (165) can also be written a

$$\left|\Delta V_k/\Delta I_k\right| \gg \left|V_k/I_k\right| \tag{169}$$

$$|\Delta V_k I_k| \gg |V_k\Delta I_k| \tag{170}$$

The critical value of ISI is 0 [61]. In the figure 4(a) the apparent power at local load bus (i.e. k) can be written as

$$S_k = V_k I_k^* \tag{171}$$

or

$$|S_k| = |V_k I_k| \tag{172}$$

Application of Taylor's theorem on eq. (172) results

$$\Delta S_k = \frac{\partial S_k}{\partial I_k}\Delta I_k + \frac{\partial S_k}{\partial V_k}\Delta V_k + \text{higher terms} \tag{173}$$

After neglecting higher order terms in eq. (173).

$$\Delta S_k = V_k\Delta I_k + I_k\Delta V_k \tag{174}$$

Within the voltage stability limit eq. (174) can be written as.

$$0 \leq 1 + \left(\frac{I_k}{V_k}\right)\left(\frac{\Delta V_k}{\Delta I_k}\right) \tag{175}$$

Linear characteristics is obtained when eq. (175) is raised to the power of α (>1). we obtain linear characteristics. Thus, without loss of generality, the VSI [63] of kth bus may be considered as follows:

$$VSI_{\text{bus}} = \left[1 + \left(\frac{I_k}{V_k}\right)\left(\frac{\Delta V_k}{\Delta I_k}\right)\right]^{\alpha} \tag{176}$$

It should be noted that VS_{Ibus} ranges from unity (no load) to zero (voltage collapse).

4) S-DIFFERENCE CRITERION (SDC)

S-difference criterion is based on two consecutive measurement of S. The power at sending end increases rapidly due to transmission losses. This increase in power at sending end does not yield an increase in useful power at receiving end. Thus, voltage collapse occurs when change in apparent power is zero (ΔS=0). New VSI is based on S-difference [64] criterion and can be written in absolute form of eq. (176) as follows:

$$SDC = \left|1 + \frac{\Delta V_k I_k^*}{V_k\Delta I_k^*}\right| \tag{177}$$

At the voltage collapse point S-difference (ΔS=0), the SDC is zero.

5) VOLTAGE COLLAPSE PREDICTION INDEX (VCPI$_k$)

For N-bus system the apparent power at kth bus can be calculated with the help of eq. (171) [65]:

$$\frac{S_k^*}{Y_{kk}} = |V_k|^2 - \left(\sum_{\substack{m=1\\ m\neq k}}^{N} \left|V_m'\right||V_k|\cos\left(\partial_k - \partial_m'\right)\right)$$

$$+j\left(\sum_{\substack{m=1\\m\neq k}}^{N}\left|V_m'\right|\left|V_k\right|\sin\left(\partial_k-\partial_m'\right)\right) \quad (178)$$

where,

$$V_m' = \frac{Y_{km}}{\sum_{\substack{j=1\\j\neq k}}^{N} Y_{kj}} V_m \quad (179)$$

Substituting ∂_k-$\partial_m' = \partial$ in eq. (178)

$$f_1\left(\left|V_k\right|,\partial\right) = \left|V_k\right|^2 - \sum_{\substack{m=1\\m\neq k}}^{N}\left|V_m'\right|\left|V_k\right|\cos\partial \quad (180)$$

$$f_2\left(\left|V_k\right|,\partial\right) = \sum_{\substack{m=1\\m\neq k}}^{N}\left|V_m'\right|\left|V_k\right|\sin\partial \quad (181)$$

At the voltage collapse point the determinant of the Jacobian matrix formed from eq. (180) & (181) should be zero. This results in eq. (182) as,

$$\frac{\left|V_k\right|\cos\partial}{\sum_{\substack{m=1\\m\neq k}}^{N} V_m'} = \frac{1}{2} \quad (182)$$

After manipulating eq. (182) and applying complex identity VCPI at k^{th} bus is obtained as:

$$VCPI_k = \left|1 - \frac{\sum_{\substack{m=1\\m\neq k}}^{N} V_m'}{V_k}\right| \quad (183)$$

The critical value of VCPI for voltage instability is 1.

6) VOLTAGE-STABILITY LOAD BUS INDEX ($VSLBI_k$)

In Figure 4(b), let the voltage across Z_{th} be ΔV_k. If load is considered as constant power type, the point of voltage collapse will be the point when maximum power is transferred. Hence, under the MPT condition, at k^{th} bus, where, $\Delta V_k = V_k$ [66], the VSLBI is defined as follows:

$$VSLBI_k = \frac{V_k}{\Delta V_k} \quad (184)$$

When, VSLBIk ≥ 1, voltage collapses.

D. P-V CURVE

Power system can be represented as in [67]:

$$\sum S_{di} + \sum S_{loss-i} = \sum S_{gi} \quad (185)$$

Subject to constraints,

$$P_{g-\min} \leq P_g \leq P_{g-\max}$$
$$Q_{g-\min} \leq Q_g \leq Q_{g-\max}$$

1) NETWORK SENSITIVITY APPROACH (SG)

Equation (185) can also be represented in active and reactive power, as

$$\left(P_{gt} + jQ_{gt}\right) = \left(P_{dt} + jQ_{dt}\right) + S_{T-loss} \quad (186)$$

where, P_{gt}: total watt power generate; Q_{gt}: total VAr power generate; P_{dt}: total watt power deman; Q_{dt}: total VAr power demand; S_{T-loss}: transmission power loss. Equation (186) can be rewritten as

$$(1 + j\alpha) P_{gt} = (1 + j\beta) P_{dt} + S_{T-loss} \quad (187)$$

where, $\alpha = Q_{gt}/P_{gt}$ and $\beta = Q_{dt}/P_{dt}$. From eq. (187) total active power generation is given by following equation:

$$P_{gt} = \frac{(1 + j\beta) P_{dt}}{(1 + j\alpha)} + \frac{S_{Loss-t}}{(1 + j\alpha)} \quad (188)$$

an

$$\frac{\partial P_{gt}}{\partial P_{dt}} = \eta \frac{P_{gt}}{P_{dt}} \quad (189)$$

where, $\eta = S_{dt}/S_{gt}$. If ≈ 0, then, the derivative of total watt power generated with respect to the total watt power demand is expressed in eq. (190).

$$S_{Gp} = \frac{\partial P_{gt}}{\partial P_{dt}} = \frac{P_{gt}}{P_{dt}} \quad (190)$$

Similarly, for reactive power give in eq. (191).

$$S_{Gq} = \frac{\partial P_{gt}}{\partial Q_{dt}} = \frac{P_{gt}}{Q_{dt}} \quad (191)$$

Equation (190) and eq. (191) can be used as a sensitivity indicator to predict voltage collapse point. As sensitivity goes to infinity system tends to voltage instability.

2) TANGENT VECTOR INDEX (TVI)

The test function in [68] may also be used for screening and ranking of contingencies for voltage stability assessment (VSA).

Network partitioning is a way to determine the weak area in a power system network for voltage collapse analysis and can also be used to define a new VSI called Tangent Vector Index (TVI) [69]. Here n-nodes may be considered as buses and C_{ij} be the connection between i^{th} and j^{th} node. Two partition techniques have been used to define and apply C_{ij} in [69]. Nature of connection between two nodes depends on the value of C_{ij}. If its value is large, it is set to be strongly connected else weakly connected.

The two techniques of partitioning are (i) Partitioning by Right Eigen vector and (ii) Partitioning by Tangent vector (TV).

The second technique is explained in [69]. The TV at the equilibrium point is equal to zero (dx/dλ=0) and is given by:

$$\left.\frac{dx}{d\lambda}\right|_* = -\left[D_x f|_*\right]^{-1} \left.\frac{\partial f}{\partial \lambda}\right|_* \tag{192}$$

The TV shows the dependency of system variable on parameter λ. The various clusters are used to define the TVI as:

$$TVI_i = \left|\frac{dV_i}{d\lambda}\right|^{-1} \tag{193}$$

The early identification of critical bus is efficiently achieved with the TV method [69], [70].

E. ENERGY FUNCTION FOR VOLTAGE STABILITY ANALYSIS

References [71] and [72] proposed the energy function for the solution of voltage instability problem.

The energy function is expressed in [73].

$$v\left(X^s, X^u\right) = \int_{(0,\theta^s,V^s)}^{(\omega,\theta^u,V^u)} \left[(M\omega)^T, f^T, g^T\right]\left[d\omega^T, d\theta^T, dV^T\right]^T \tag{194}$$

In eq. (194), (ω, θ^u,V^u) and (0, θ^s,V^s) represent solutions at equilibrium state; ω^T =[ω_1,......ω_m]: velocity matrix; V^T =[V_1.....V_n]: voltage matrix, and θ^T =[θ_1..... θ_n]: phase angle matrix; M is the inertia matrix; f^T =f(θ, V) and g^T =g(θ,V) may be expressed as:

$$f_i(\theta, V) = P_i - \sum_{j=1}^{n} B_{ij} V_i V_j \sin\left(\theta_i - \theta_j\right) \tag{195}$$

$$g_i(\theta, V) = (V_i)^{-1}\left[Q_i(V_i) + \sum_{j=1}^{n} B_{ij} V_i V_j \cos\left(\theta_i - \theta_j\right)\right] \tag{196}$$

Equation (194) defines Lyapunov function considering that Watt power injections are constant; VAr power injections and transfer conductance's are neglected.

Equation (194) can be extended into kinetic & potential energy as:

$$v\left(X^s, X^u\right)$$
$$* = \overbrace{\frac{1}{2}\omega^T M\omega}^{KineticEnergy} + \left[\overbrace{\begin{array}{l} -\sum_{i=1}^{n}\int_{V_i^s}^{V_i^u}\frac{Q_i(V_i)}{V_i}dV_i - \sum_{i=1}^{n} P_i\left(\theta_i^u - \theta_i^s\right) \\ -\frac{1}{2}\sum_{i=1}^{n}\sum_{j=1}^{n} V_i^u V_j^u B_{ij}\cos\left(\theta_i^u - \theta_j^u\right) \\ +\frac{1}{2}\sum_{i=1}^{n}\sum_{j=1}^{n} V_i^s V_j^s B_{ij}\cos\left(\theta_i^s - \theta_j^s\right) \end{array}}^{PotentialEnergy}\right] \tag{197}$$

Equation (197) shows the sum of kinetic & potential energy. Potential energy is completely dedicated to show the weakness to steady state voltage instability.

Equation (195) and (196) after introduction of transfer conductance are follows:

$$f_i(\theta, V) = P_i - \sum_{j=1}^{n} B_{ij} V_i V_j \sin\left(\theta_i - \theta_j\right) - \sum_{j=1}^{n} G_{ij} V_i^s V_j^s \cos\left(\theta_i^s - \theta_j^s\right) \tag{198}$$

$$g_i(\theta, V) = (V_i)^{-1}\left[Q_i(V_i) + \sum_{j=1}^{n} B_{ij} V_i V_j \cos\left(\theta_i - \theta_j\right)\right] - \left(V_i^s\right)^{-1}\sum_{j=1}^{n} G_{ij} V_i^s V_j^s \cos\left(\theta_i^s - \theta_j^s\right) \tag{199}$$

Now eq. (194) can be rewritten as:

$$v\left(X^s, X^u\right) = \sum_{i=1}^{n}\left[\int_{\theta_i^s}^{\theta_i^u} f_i(\theta, V)\, d\theta_i + \int_{V_i^s}^{V_i^u} g_i(\theta, V) dV_i\right] \tag{200}$$

The assessment of the above equation results in:

$$\begin{aligned} v\left(X^s, X^u\right) = &-\sum_{i=1}^{n}\int_{V_i^s}^{V_i^u}\frac{Q_i(V_i)}{V_i}dV_i - \sum_{i=1}^{n} P_i\left(\theta_i^u - \theta_i^s\right) \\ &-\frac{1}{2}\sum_{i=1}^{n}\sum_{j=1}^{n} V_i^u V_j^u B_{ij}\cos\left(\theta_i^u - \theta_j^u\right) \\ &+\frac{1}{2}\sum_{i=1}^{n}\sum_{j=1}^{n} V_i^s V_j^s B_{ij}\cos\left(\theta_i^s - \theta_j^s\right) \\ &+\sum_{i=1}^{n}\sum_{j=1}^{n} V_i^s V_j^s G_{ij}\cos\left(\theta_i^s - \theta_j^s\right)\left(\theta_i^u - \theta_j^s\right) \\ &+\sum_{i=1}^{n}\sum_{j=1}^{n} V_j^s G_{ij}\sin\left(\theta_i^s - \theta_j^s\right)\left(V_i^u - V_j^s\right) \end{aligned} \tag{201}$$

The energy function described by eq. (201) can be used for determination of voltage security indices [74], [75].

F. MODEL ANALYSIS FOR VOLTAGE STABILITY EVOLUTION

Since at any bus, voltage is dependent on VAr power at that bus, V-Q sensitivity can be utilized to determine the stability of the system. If it is positive, system will be stable else unstable [76].

1) REDUCED JACOBIAN MATRIX

The relation between power & voltage may be given by:

$$\begin{bmatrix}\Delta P \\ \Delta Q\end{bmatrix} = \begin{bmatrix} J_{P\theta} & J_{PV} \\ J_{Q\theta} & J_{QV}\end{bmatrix}\begin{bmatrix}\Delta\theta \\ \Delta V\end{bmatrix} \tag{202}$$

Voltage stability of any power system network depends on Watt and VAr power. In Q-V curve approach, the Watt power is considered constant and VSA is done by incremental relationship between V & Q.

$$\Delta Q = \left[J_{QV} - J_{Q\theta} J_{P\theta}^{-1} J_{PV} \right] \Delta V = J_R \Delta V \tag{203}$$

and

$$\Delta V = J_R^{-1} \Delta Q \tag{204}$$

where,

$$J_R = \left[J_{QV} - J_{Q\theta} J_{P\theta}^{-1} J_{PV} \right] \tag{205}$$

where J_R: reduced Jacobian matrix

2) MODES OF VOLTAGE INSTABILITY

Assuming,

$$J_R = \xi \wedge \eta \tag{206}$$

where, ξ =column vector matrix of J_R, η = row vector matrix of J_R and ^= diagonal Eigen value matrix of J_R. And

$$J_R^{-1} = \xi \wedge^{-1} \eta \tag{207}$$

From eq. (204) and eq. (207)

$$\Delta V = \xi \wedge^{-1} \eta \Delta Q \tag{208}$$

or

$$\Delta V = \sum_i \frac{\xi_i \eta_i}{\lambda_i} \Delta Q \tag{209}$$

Each eigenvalue is represented by λ_i and the corresponding column and row eigenvectors are represented by ξ_i and η_i, respectively. The i_{th} nodal Reactive power difference is given by:

$$\Delta Q_{mi} = k_i \xi_i \tag{210}$$

where,

$$k_i^2 \sum_j \xi_{ji}{}^2 = 1 \tag{211}$$

The corresponding i^{th} node voltage difference is given by:

$$\Delta V_{mi} = \frac{1}{\lambda_i} \Delta Q_{mi} \tag{212}$$

n-node power system network consists of n values of λ. The value of each λ corresponds to the strength of that node to the voltage stability. If λ for i^{th} bus is zero then it shows that i^{th} bus is responsible for system voltage collapse [76].

The VSIs presented in this section may be classified based on line, bus and system parameters, their applicability to transmission and distribution networks and basic concepts. Figure 5 presents a classification of indices based on their applicability to transmission and distribution systems. The indices that are suitable for the transmission system may be utilized in the planning of control measures such as the placement of Flexible AC Transmission System (FACTS) Controllers. The indices suitable for distribution systems may be utilized for the optimal placement of distributed generations and may be quite helpful in demand-side management. Table 2 classifies indices to identify critical buses and lines that need special attention to prevent voltage instability-driven blackouts. Accordingly, proper planning of compensating devices and remedial measures may be decided.

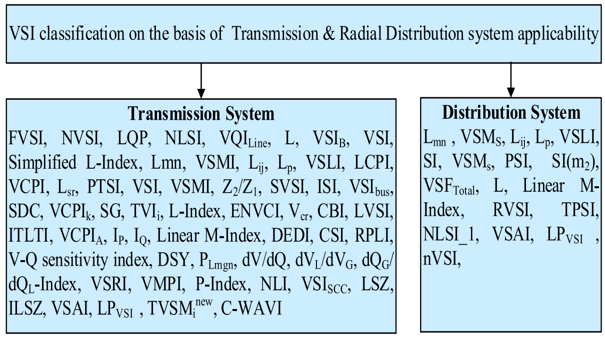

FIGURE 5. VSIs classified on the basis of their applicability to transmission & distribution system.

IV. NOVEL QUALITATIVE COMPARISON OF VOLTAGE STABILITY INDICES

VSIs are difficult to compare quantitatively due to varied approach and applications, Hence, they may be qualitatively compared on the basis of their complexity, accuracy, time, mode of operation (i.e. online/offline), data dependency, and type of stability (steady state/transient or dynamic).

A. COMPLEXITY

The complexity of a Variable Step-Size Incremental (VSI) algorithm is contingent upon the analysis of the data collection process and the computational complexity involved. Data collection, data aggregation, and data selection are distinct procedures involved in the processing of data. Data collection involves the acquisition of data pertaining to each bus and line within the power system network. This is accomplished by utilizing sensing devices such as ammeters, voltmeters, wattmeters, and/or phasor measurement units (PMUs). Further, Data aggregation is performed on the collected data to reduce error [124]. Finally, Data selection depends on the VSI technique used.

However, the data obtained from the abovementioned process is erroneous & may affect the VSIs deduction. Absolutely, at different levels, PMU data loss occurs in the different practical applications due to delay in transmission of data, hardware failure and communication congestion etc. Noise in PMU data and PMU data loss as expected reduce the performance and reliability of the voltage stability indices.

Researchers mainly try to reduce the code length for the purpose of reducing memory storage of the algorithm. But on other hand it reflects in complexity of algorithm. Few algorithms take more time and memory storage for solving the voltage stability problem. In real time calculation the response time is the deciding factor as time taken beyond the permissible value may result in instability. Memory storage

TABLE 2. Summary of voltage stability indices along with their features.

S. No.	Index	Abbreviation	References	Critical value	Stability Condition	Equation	Assumption	VSI Type
1	L_{mn}-Index	L_{mn}	[77] [78]	1	L_{mn} <1 stable L_{mn} >1 unstable	$L_{mn} = \frac{4XQ_2}{[V_1 \sin(\theta - \partial)]^2}$	A_1, A_2	Line
2	L_{ij}-Index	L_{ij}	[79]	1	L_{ij} <1 stable L_{ij} >1 unstable	$L_{ij} = \frac{4Z^2 Q_2 X}{V_1^2 (R \sin\partial + X \cos\partial)^2}$	A_1	Line
3	Fast voltage stability index	FVSI	[80]	1	FVSI<1 stable FVSI> unstable	$FVSI = \frac{4Z^2 Q_2}{V_1^2 X}$	A_1, A_4	Line
4	New voltage stability index	NVSI	[81]	1	NVSI<1 stable NVSI>1unstable	$NVSI = \frac{2X\sqrt{P_2^2 + Q_2^2}}{2Q_2 X - V_1^2}$	A_1, A_5	Line
5	Line stability factor	LQP	[40] [82]	1	LQP<1 stable LQP>1 unstable	$LQP = 4\left[\frac{X}{V_1^2}\right]\left[\frac{X}{V_1^2}P_1^2 + Q_2\right]$	A_1, A_5	Line
6	Line stability index	L_p	[41] [83]	1	L_p <1 stable L_p >1 unstable	$L_P = \frac{4RP_2}{V_1^2 \cos^2(\theta - \partial)}$	A_1, A_3	Line
7	New line stability index	NLSI	[42] [84]	1	NLSI<1 stable NLSI>1 unstable	$NLSI = \frac{RP_2 + XQ_2}{0.25V_1^2}$	A_1, A_4	Line
8	Voltage reactive power index	VQI_{Line}	[43]	1	VQI_{Line} <1 stable VQI_{Line}>1unstable	$VQI_{Line} = \frac{4Q_2}{B_{12}V_1^2}$	A_1, A_4	Line
9	Voltage stability load index	VSLI	[44] [45]	1	VSLI<1 stable VSLI>1 unstable	$VSLI = \frac{4\left[V_1^2\left(P_2R + Q_2X\right) + \left(P_2R + Q_2X\right)^2\right]}{V_1^4}$	A_1	Line
10	L-index	L	[46]	1	L<1 stable L>1 unstable	$L = \frac{4\left[V_1V_2 - V_2^2\right]}{V_1^2}$	A_1, A_4	Line
11	Voltage stability indicator	VSI_B	[47]	1	VSI_B <1 stable VSI_B>1 unstable	$VSI_B = \frac{4Q_2\left(R + X\right)^2}{X\left(V_1^2 + 8RQ_2\right)}$	A_1, A_4	Line
12	Stability index	SI	[48]	0	SI≠0 stable SI≠0 unstable	$SI = 2V_1^2V_2^2 - V_2^4 - 2V_2^2\left(P_2R + Q_2X\right)$ $-\lvert Z\rvert^2\left(P_2^2 + Q_2^2\right)$	A_1	Line
13	Line collapse proximity index	LCPI	[49]	1	LCPI<1 stable LCPI>1 unstable	$LCPI = \frac{4\left(A\cos\alpha\right)\left(P_2B\cos\beta + Q_2B\sin\beta\right)}{\left(V_1\cos\partial\right)^2}$	A_6	Line
14	Voltage collapse proximity indicator	VCPI	[35]	1	VCPI<1 stable VCPI>1unstable	$VCPI(1) = \frac{P_2}{P_{2(\max)}}, VCPI(2) = \frac{Q_2}{Q_{2(\max)}}$ $VCPI(3) = \frac{P_l}{P_{l(\max)}}, VCPI(4) = \frac{Q_l}{Q_{l(\max)}}$	A_1, A_7	Line
15	L_{sr}-Index	L_{sr}	[51]	1	L_{sr} <1 stable L_{sr} >1 unstable	$L_{sr} = \frac{S_2}{S_{2(\max)}} \quad S_{r(\max)} = \frac{V_s^2}{4Z\cos^2\left(\frac{\theta - \phi}{2}\right)}$	A_1, A_7	Line

TABLE 2. ***(Continued.)*** **Summary of voltage stability indices along with their features.**

16	Power system stability index	PTSI	[52]	1	PTSI<1 stable PTSI>1 unstable	$PTSI=\frac{2S_2Z_1\left(1+\cos(\theta-\phi)\right)}{V_1^2}$	A_1	Line
17	Voltage stability index	VSI	[53]	0	VSI>0 stable VSI<0 unstable	$VSI=\min\left(\frac{P_{margin}}{P_{2(\max)}},\frac{Q_{margin}}{Q_{2(\max)}},\frac{S_{margin}}{S_{2(\max)}}\right)$	A_1, A_5, A_7	Line
18	Voltage stability margin	VSM_s	[54]	0	VSM_s >0 stable VSM_s<0unstable	$VSM_s=\frac{S_{cr}-S_2}{S_{cr}}$ $S_{cr}=\frac{V_s^2}{2Z\left[1+\cos(\theta-\phi)\right]}$	A_1, A_7	Line
19	Voltage stability margin index	VSMI	[55] [85]	0	VSMI>0 stable VSMI<0unstable	$VSMI=\frac{\partial_{\max}-\partial}{\partial_{\max}}$	A_1	Line
20	Z_2/Z_1-Index	Z_2/Z_1	[57]	1	Z_2/Z_1 >1 stable Z_2/Z_1<1unstable	$\frac{Z_2}{Z_1}=\frac{M+1}{-M\cos\partial+\sqrt{\left[(M\cos\partial)^2-M^2+1\right]}}$ $M=\frac{(S_2-S_1)(Y_2+Y_1)}{(S_2+S_1)(Y_2-Y_1)}$	A_7	Bus
21	Simplified voltage stability index	SVSI	[58] [59] [60]	1	SVSI≠1 stable SVSI=1 unstable	$SVSI=\frac{\Delta V_i}{\beta V_i}$	A_8	Bus
22	Impedance-stability index	ISI	[61]	0	ISI≈1 stable ISI≈0 unstable	$ISI=\frac{\left(\hat{Z}_k-\hat{Z}_{th}\right)}{\hat{Z}_k}$ or $ISI=1-\lvert I_k\Delta V_k\rvert/\lvert V_k\Delta I_k\rvert$	A_{10}	Bus
23	Bus VSI	VSI_{bus}	[63]	0	VSI_{bus} ≠0 stable VSI_{bus}=0unstable	$VSI_{bus}=\left[1+\left(\frac{I_k}{V_k}\right)\left(\frac{\Delta V_k}{\Delta I_k}\right)\right]^{\alpha}$	A_{11}	Bus
24	S-difference criterion	SDC	[64]	0	SDC≠0 stable SDC= unstable	$SDC=\left\lvert 1+\frac{\Delta V_k I_k^*}{V_k\Delta I_k^*}\right\rvert$	A_{11}	Bus
25	Voltage collapse prediction index	$VCPI_k$	[65]	1	$VCPI_k$ =0 stable $VCPI_k$=1unstable	$VCPI_k=\left\lvert 1-\frac{\sum_{m=1,\,m\neq k}^{N}V_m'}{V_k}\right\rvert$	A_{12}	Bus
26	Voltage-stability load bus index	$VSLBI_k$	[66]	1	$VSLBI_k$ >1 stable $VSLBI_k$<1 unstable	$VSLBI_k=\frac{V_k}{\Delta V_k}$	A_{13}	Line
27	Network sensitivity approach-based index	SG	[67]	Sharp rise	Gradual increase	$S_{Gp}=P_{gt}/P_{dt}$ $S_{Gq}=P_{gt}/Q_{dt}$	A_9	Over all
28	Test function	TF	[86]	Details are given in the reference.		$t=e_l^tJ(x,y)v$	-	Bus
29	Tangent vector index	TVI_i	[69]	0	TVI_i ≠ stable TVI_i =0 unstable	$TVI_i=\left\lvert\frac{dV_i}{d\lambda}\right\rvert^{-1}$	-	Bus
30	L-index	L-Index	[87]	1	L<1 stable L>1 unstable	$L=\underset{j\in\alpha_L}{MAX}\left\lvert 1-\frac{\sum_{i\in\alpha_G}F_{ji}V_i}{V_J}\right\rvert$	$V_{\alpha G}$:fixed	Bus
31	Power stability index	PSI	[42]	1	PSI<1 stable PSI>1 unstable	$PSI=\frac{4r_{ij}(P_L-P_G)}{\left[\lvert V_i\rvert\cos(\theta-\delta)\right]^2}$	r_{IJ}≠0	Bus

TABLE 2. ***(Continued.)*** **Summary of voltage stability indices along with their features.**

32	Voltage deviation index	VDI_T	[38]	Details are given in the reference.		$VDI_T = \sum_{j=1}^{N} \lvert 1 - V_j \rvert$	-	Bus
33	Stability index	$SI(m_2)$	[88]	0	$SI(m_2) \geq 0$ stable, Unstable otherwise	$SI(m_2) = \{\lvert V(m1)\rvert^4 - 4\{P(m2)x(jj) - Q(m2)x(jj)\}\}^2 - 4\{P(m2)r(jj) + Q(m2)x(jj)\}\lvert V(m1)\rvert^2$	$r_{IJ} \neq 0$	Bus
34	Equivalent node voltage collapse index	ENVCI	[69] [89]	0	0: unstable 1: stable	$ENVCI = 2(e_k e_n + f_k f_n) - (e_k^2 + f_k^2)$	A_{14}	Bus
35	Voltage stability factor	VSF_{total}	[90]	1	$VSF_{total} > 1$: stable $VSF_{total} < 1$: unstable	$VSF_{total} = \sum_{m=1}^{k-1} (2V_{m+1} - V_m)$	-	Bus
36	L-index	L-Index	[27]	-	-	$L = 4\left[(xP_L - rQ_L)^2 + xQ_L - rP_L\right]$ For L<1 $L = 4\left[(x_{eg}P_{leg} - r_{eg}Q_{leg})^2 + x_{eg}Q_{leg} - r_{eg}P_{leg}\right]$	-	-
37	Voltage instability proximity index	VIPI	[27]	-	-	$VIPI = \theta = \cos^{-1} \frac{\Upsilon_S^T \Upsilon(a)}{\lVert\Upsilon_S\rVert \lVert\Upsilon(a)\rVert}$	-	-
38	Integral steady state margin	ISSM	[27]	b/t 0&1	$0 < ISSM < 1$	$ISSM = \left\lvert \frac{J_C}{J_0} \right\rvert$	-	-
39	Critical voltage	V_{cr}	[27]	The critical value of voltage	-	$V_{cr} = \frac{E}{\sqrt{2(1 + \cos(\alpha - \phi))}} = \frac{E}{2\cos\theta}$	-	Bus
40	Critical boundary index	CBI	[81]	0	CBI>0: stable Unstable otherwise	$CBI_{ik} = \sqrt{\Delta P_{ik}^2 + \Delta Q_{ik}^2}$ $\Delta P_{ik} = X - P_0$ $\Delta Q_{ik} = Y - Q_0$	-	Line
41	Line voltage stability index	LVSI	[91]	1	LVSI=1: unstable $1 < LVSI < 2$: stable	$LVSI = \max(LVSI_j) \quad \forall j = 1,2,3....l$	-	Line
42	Integrate transmissio n line transfer index	ITLTI	[92]	1	ITLTI<1: stable ITLTI≥1: unstable	$S_{R\_Index} = \frac{\sin(\theta_R + \delta)\sin\delta}{\cos\left(\theta_R/2\right)}$	A_{15}	Line
43	Voltage collapse proximity indicator	$VCPI_A$	[93] [94]	0	$VCPI_A$ ≥stable $VCPI_A$ <0unstable	$VCPI_A = V_2\cos(\delta) - 0.5V_1$	A_8	Line
44	Linearized motor voltage stability index	LMVSI	[15]	-	-	$LMVSI_i = \frac{MVSI_i}{\lvert d(MVSI_i)/d\lambda_i \rvert}$ $MVSI = \lvert \det(A_i) \rvert,\ \lambda_i = (P_L^{t_i} - P_L^{t_0})/P_L^{t_0}$	A_{16}	Bus
45	Simplified L-index	L'	[95]	1	L'<1: Stable L'>1: unstable	$L_j = \frac{1}{V_j^2}\sqrt{f'^2 + g'^2}$ $f_i' = Q_i X_{ij},\ g_i' = -P_i X_{ij}$	A_4, A_5	Bus
46	MW & MVar dispatch index	I_P and I_Q	[14]	-	-	$I_P = \frac{\Delta l}{\Delta C_i} = \frac{n_{pi}}{n_p^T P_l + n_Q^T Q_l}$	-	Bus

TABLE 2. ***(Continued.)*** **Summary of voltage stability indices along with their features.**

						$I_Q = \frac{\Delta l}{\Delta C_i} = \frac{n_{Qi}}{n_p^T P_l + n_Q^T Q_l}$		
47	Linear M-index	M	[96] [97]	0	0: stability limit point	$M - index = 1 - \frac{P}{P_{cr}}$	-	Bus
48	Diagonal element dependent index	DEDI	[98] [99]	-	-	$I_{qi} = \frac{\partial Q_i / \partial V_i}{-B_{ii}}; I_{pi} = \frac{\partial P_i / \partial \delta_i}{-B_{ii}}; I_i = \frac{\partial P_i / \partial \delta_i}{\sum_{i=1, j \neq 1}^{N} B_{ii} V_j}$	-	Bus
49	Revamp voltage stability indicator	RVSI	[100] [101]	1	RVSI=1: unstable otherwise stable	$RVSI = \frac{4 Z_{ij}^2 Q_r X_{ij}}{V_s^2 \left(R \sin \delta + X \cos \delta \right)^2}$	A_1	Line
50	Composite severity index	CSI	[13] [98] [99]	1	CSI<1: stable CSI>1: unstable	$CSI = w_1 * \frac{w_{mn}}{2a} \left(\frac{P_{mn}}{P_{mn}^{max}} \right)^{2a} + w_2 * \frac{4 x Q_n}{\left[V_m \sin(\theta - \delta) \right]^2}$	A_{17}	Line
51	Reactive power loss index	RPLI	[104] [105]	Highest value to weakest bus	Lowest RPIL is more stable	$RPIL_i = Qloss_{i,0}^n + \sum Qloss_{i,k}^n * NCOSI_k$	-	Bus
52	V-Q sensitivity index	S_Q^V	[106]	-	Depends on cut-off value	$S_Q^V = \left\{ \max_{i=1,\dots,n} \left[diag\left(J_{Ri}^{-1}\right)\Big\|_{t2} - diag\left(J_{Ri}^{-1}\right)\Big\|_{t1} \right] * 10$	A_{18}	Bus
53	D_v^{ij}-index	D_v^{ij}	[107]	1	0< D_v^{ij} <1	$D_v^{ij} = \frac{V_i}{\sqrt{2V_j^2 + 2\left(P_j' R + Q_j' X\right)}}$	A_{19}	Line
54	Derivative of load with respect to Y	DSY	[12]	0	DSY: +ve stable DSY: -ve unstable	$DSY = \frac{\Delta S_t}{V_l^2 \Delta Y_l}$	A_{20}	Bus
55	Short term voltage stability index	$SVSI_r$ $SVSI_0$ $SVSI_s$	[108]	-	-	$SVSI_r = \int_{T_{Flt}}^{SVSI_r} \left\| v(t) - V_s \right\| dt$ $SVSI_0 = \int_{t_{Clear}}^{t_{End}} \left\| v_{TVSI_0}(t) - v(t) \right\| dt$ $SVSI_s = \left(v(0) - V_s \right) * (t_{Stable} - t_{Clear})$	A_{21}	Bus
56	Contingency ranking index	M_i^o, M_i^j	[11]	-	-	$M_i^0 = S_{m_i}^0 - S_i^0$ $M_i^j = S_{m_i}^j - S_i^j$	-	Bus
57	Influence index	II_i^j	[11]	0	II -ve: severe disturbance	$II_i^j = (signof\ \beta_i^o) * \left(\frac{M_i^j}{M_i^0} - 1 \right)$	-	Bus
58	Active power load margin	P_{Lmgn}	[109]	0	0< P_{Lmgn} <1	$P_{Lmgn} = \frac{P_{max\ n} - P_0}{P_{max\ n}}$	A_7	Bus
59	Voltage collapse sensitivity index	dV/dQ-Index	[110]	-	0<index<∞	$I_i = \Delta \sum_{J \in L} \frac{Q_j}{V_i} \frac{\delta V_i}{\delta Q_j}, i \in L$	-	Bus
60		dV_L/dV_G-Index	[110]	∞	At infinity system collspse	$J_i = \Delta \sum \frac{\delta V_i}{\delta V_k}, i \in L$	-	Bus

TABLE 2. ***(Continued.)*** **Summary of voltage stability indices along with their features.**

61		dQ_G/dQ_L-Index	[110]	-∞	$-\infty<K_i<-1$	$K_i=\Delta\sum_{K\in G}\frac{\delta Q_k}{\delta Q_i}, i\in L$	-	Bus
62	Transmission path stability index	TPSI	[10] [111]	0	TPSI=0 For unstable system	$TPSI=0.5V_i-v_d$	A_{20}	Line
63	Voltage stability predictor	VIP	[9]	0	ΔS=0 for unstable system	$\Delta S=\frac{\left(V_j-Z_{th}I_{ij}\right)^2}{4Z_{th}}$	-	Bus
64	New line stability index	NLSI_1	[112]	1	NLSI_1<1: stable NLSI_1>1: unstable	$NLSI\_1=\frac{4q}{\lvert V_s\rvert^2}\left[\frac{\lvert Z\rvert^2}{X}\sigma-\frac{X}{\sin^2(\theta-\delta)}(\sigma-1)\right]$	$\partial_r-\partial_s\neq0$	Line
65	Voltage stability risk index	VSRI	[8] [113]	-ve value	VSRI<0 bus will be more unstable	$VSRI_j=\frac{1}{N}\left[\frac{\sum_{i=j+N-1}^{j}(d_i+d_{i-1})\Delta t}{2}\right]$	-	Bus
66	Voltage margin proximity index	VMPI	[114] [7]	-	-	$VMPI=\theta=\begin{cases}\cos^{-1}\frac{V^t*V_L}{\lVert V\rVert*\lVert V_L\rVert}(\lVert V\rVert>\lVert V_L\rVert)\\-\cos^{-1}\frac{V^t*V_L}{\lVert V\rVert*\lVert V_L\rVert}(\lVert V\rVert<\lVert V_L\rVert)\end{cases}$	-	-
67	Approximate collapse power index	ACPI	[115]	1	0<ACPI<1: stable ACPI=1: unstable	$ACPI=\frac{P_{iA}}{P_{C,i}}$ $ACPI=\frac{1}{1+d\lambda_{C,i}}$	2nd order approximation	Bus
68	P-Index	P-Index	[4] [116]	1	P-Index: unstable	$P-Index=-\frac{\frac{P_L}{V}\frac{dV}{dP_L}}{1-2\frac{P_L}{V}\frac{dV}{dP_L}}$	A_7	Bus
69	New LIVES index	NLI	[5]	0	NLI>0: stable	$NLI=\frac{\Delta P}{\Delta G_P}$	A_7	Bus
70	VSI based on SCC	VSI_{SCC}	[6]	1	$VSI_{SCC}<1$: stable $VSI_{SCC}>1$: unstable	$VSI_{SCC}=\frac{SCC_{\min}}{SCC_p}=\frac{2S_LX_{th}(1+\sin\phi)}{E^2{}_{th}}$	A_8	Line
71	Line stability index	LSZ	[117]	1	LSZ>1 unstable LSZ<1 stable	$LSZ=\frac{2\lvert Z\rvert\lvert S_r\rvert}{\lvert V_s\rvert^2-2\lvert Z\rvert(P_r\cos\theta+Q_r\sin\theta)}$	A_1	Line
72	Improved LSZ	ILSZ	[117]	1	ILSZ>1unstable ILSZ<1 stable	$ILSZ=\frac{2\lvert Z+Z_{th}\rvert\lvert S_r\rvert}{\lvert E_s\rvert^2-2\lvert Z+Z_{th}\rvert(P_r\cos\theta+Q_r\sin\theta)}$	A_1	Line
73	Voltage stability assessment index	VSAI	[118]	1	VSAI> unstable VSAI<1 stable	$VSAI=\frac{p}{\bar{p}_{\max}}$ $p=P_r/P_{rB},\ P_{rB}=\frac{RV_{ref}^2}{R^2+X^2}$	A_1	Bus
74	Load pattern based VSI	LP_{VSI}	[119]	1	$LP_{VSI}>1$unstable $LP_{VSI}<1$ stable	$LP_{VSI}=e^{-(((V^2{}_{th_x}+V^2{}_{thy})(\lvert R_{th}\rvert+\lvert X_{th}\rvert)/(4(R_{th}^2+X_{th}^2)))}$	A_1	Bus
75	Thevenin based voltage stability margin	$TVSM_i^{new}$	[120]	0	TVSM>0stable TVSM<0unstable	$TVSM_i^{new}=\frac{\lvert Z_{eq,i}\rvert}{\lvert Z_{L,i}\rvert},\ \lvert Z_{eq,i}\rvert=\lvert Z_{L,i}\rvert-\lvert Z_{eq,i}^{new}\rvert$ $Z_{eq,i}^{new}=Z_{eq.i}+Z_{a,i}$	A_1	Bus

TABLE 2. ***(Continued.)*** **Summary of voltage stability indices along with their features.**

76	New VSI	$_n$VSI	[121]	0	$_n$VSI=0 stable $_n$VSI=1 unstable	$_nVSI=\frac{4R_iP_i^2}{(Q_iV_{i-1}\sin\delta_i+P_iV_{i-1}\cos\delta_i)^2}\left(P_i+\frac{Q_i^2}{P_i}\right)$	A_1	Line
77	Constancy enhanced wide area VSI	C-WAVI	[122]	1	1=unstable <1=stable	$C-WAVI=\frac{\lvert S_{eq}\rvert}{\lvert S_{eq,\max}\rvert}=\left(\frac{2k+2k\cos(\theta-\phi)}{1+k^2+2k\cos(\theta-\phi)}\right)$ where, $k=\frac{\lvert Z_{th}\rvert}{\lvert Z_{app}\rvert}$	A_1	Line
78	Line Voltage Collapse Index (LVCI)	LVCI	[123]	1	2=stable 1=unstable	$(LVCI)_k=\frac{2V_jA_k\sin(\beta_k-\alpha_k)}{V_i\sin(\beta_k-\delta_k)}$	-	Line

is also a concern for large power system networks. If VSI requires huge amount of dataset of independent variables it will consume more storage that creates problem when power system network is large.

As per above discussion complexity basically depends on data collection, data aggregation and data selection. Here in qualitative comparison if the VSI depends on two system variables the complexity is assumed as low; if it depends on three system variables the complexity is assumed as medium and if it depends on more than three system variables the complexity of the VSI is assumed as high with all other conditions assumed to be same.

B. EFFICACY

Efficacy of VSIs depends on the number of approximations incorporated during mathematical derivation. Lower number of approximations results in better accuracy. Various assumptions found in literature have been summarized in the Table 1 with justification and applicability. Furthermore, the level of efficiency is contingent upon the specific Variable Speed Drive Interface (VSI) employed. Static voltage stability indices (VSIs) are dependent on load flow models, which might potentially result in imprecise outcomes due to their disregard for dynamic elements such as the low inertia compressor motor of air conditioners, heating pumps, and refrigerators. Additionally, efficacy depends on the data used for calculating purposes.

Generally, efficacy of VSI highly depends on total number of approximations taken during derivation of that VSI. Here in qualitative analysis if approximation taken in the derivation of VSI is only one its efficacy is assumed as high, if number of approximations are two, efficacy of VSI is assumed as medium and if approximation taken are more than two, efficacy of VSI is assumed as low.

C. COMPUTATIONAL TIME

Computational time of any VSI includes processing time and data collection and communication delay. Independent variables are measured through sensing devices and shared to processing unit through communication channels. Thus, there shall be a time lag between data transmission and reception. There are several data measuring and data sensing devices like ammeter, voltmeter, wattmeter and PMUs. Measured or sensed data from these devices is sent to data concentration unit and from there it is sent to the processing unit. All the data is transmitted from one place to other through communication channels and takes some finite time to reach the computation unit. In addition to this the computation unit shall also consume some processing time depending on the VSI selected.

D. MODE OF OPERATION

VSIs are computed in online/offline mode. In online mode, VSI are calculated in real time and give response instantly for performing immediate corrective measures. Variable-based voltage stability indices (VSIs) that rely on the admittance matrix [Y_{BUS}] and system variables like bus voltages or power flow across lines are computationally efficient and suitable for online monitoring. One limitation of these indices is their inability to provide an exact estimation of the actual margin from voltage collapse. Nonetheless, they are capable of identifying essential lines and buses. Offline VSI assessment is basically done for planning and analysis purpose. Accurate calculation of VSIs in offline mode is a major concern. Time is not as critical parameter for offline mode as it is in online VSA.

E. TYPE OF VOLTAGE STABILITY

The examination of voltage stability can be broadly classified into two categories: large-disturbance voltage stability, also known as transient voltage stability, and small-disturbance voltage stability, also known as steady-state voltage stability. The occurrence of significant voltage instability is attributed to the presence of substantial disturbances, such system faults, generation loss, or circuit contingencies. Small voltage instability caused by small disturbances can occur due to minor perturbations, such as gradual variations in the load of a system.

A comparative overview of voltage stability indices presented in this paper has been shown in Table 3. In Table 3,

TABLE 3. Comparative analysis of VSIs on the basis of applications, accuracy, mode of operation, variation of VSI with respect to system parameter and type of stability calculation.

S. No.	VSI	Applications	Accuracy	Offline /Online	Complexity	System Parameter	Stability
1	L_{mn}	Online monitoring of power system stability Contingency monitoring and voltage collapse prediction	Medium	Online	High	Active load change	Transient
2	L_{ij}	Determining voltage stability limit. Weak area clustering. Optimal Location and Sizing of Reactive Power Compensation	High	Offline	High	Reactive load change	Steady state
3	FVSI	Find the weakest line. Quantitative assess the voltage stability.	Medium	Online	Medium	Load changes	Transient
4	NVSI	Voltage stability analysis on power grid with integrated distributed generation system.	Medium	Offline	Medium	Load change	Steady state
5	LQP	Optimal location for the placement of UPFC device	Medium	Offline	Medium	Load change	Steady state
6	L_p	Assessment of Voltage Stability in Ill-Conditioned Radial Distribution Network	Medium	Offline/ online	High	Load change	Steady state /Transient
7	NLSI	Voltage stability assessment.	Medium	Offline	Medium	Load change	Steady state
8	VQI_{Line}	Voltage stability assessment.	Medium	Offline	Medium	Load factor	Steady state
9	VSLI	Voltage stability assessment in radial distribution system. Online voltage stability assessment using PMU data	High	Offline/Online	High	Receiving end load PMU data	Steady state
10	L	Voltage stability monitoring of power system network.	Medium	Offline/Online	Low	Receiving end load PMU data	Steady state
11	VSI_B	Voltage stability analysis of power system	Medium	Offline	Medium	Loading condition	Steady state
12	SI	Voltage stability analysis of distribution network. Optimal allocation and sizing and siting of DG.	High	Offline	Medium	Loading conditions for different static load models	Steady state
13	LCPI	Voltage stability assessment under all operating conditions.	High	Offline	High	Load multiplier factor	Steady state
14	VCPI	Real-time contingency evaluation and ranking.	Medium	Online	Low	System parameters, network topology, interconnections and load demand of the system.	Steady state
15	L_{sr}	Voltage stability assessment in real time operation of power systems Contingency ranking	Medium	Offline	Low	Load at bus	Steady state
16	PTSI	Predicting dynamic voltage collapse.	High	Offline	Medium	Reactive load	Dynamic
17	VSI	Online voltage stability assessment.	Low	Online	Low	PMU data and load parameters	Steady state
18	VSM_s	Voltage stability analysis for distribution system connected to transmission network.	Medium	Online	High	Loading factor	Dynamic
19	VSMI	Identification of Weak Locations in Bulk Transmission Systems in real time.	High	Offline	Low	Angle difference between sending and receiving end buses	Steady /Dynamic
20	Z_2/Z_2	Load shedding.	High	Offline	Low	Load and admittance at the end of change	Steady state
21	SVSI	Online and in real time voltage stability monitoring with the help of PMU data.	High	Online	Low	PMU and relative electrical distance (i.e. the location of generator near to the load bus)	Steady state
22	ISI	Used in wide area monitoring May be used locally in numerical relay.	High	Online	Low	PMU data Thevenin's parameters	Steady state
23	VSI_{bus}	Determine margin to voltage collapse.	High	Offline	Medium	Voltage and currents through the results of power flow	Steady state
24	SDC	Local phasor-based voltage collapse protection.	Medium	Online/ Offline	Low	Change in apparent power in a line at two different intervals of time.	Steady state

TABLE 3. *(Continued.)* **Comparative analysis of VSIs on the basis of applications, accuracy, mode of operation, variation of VSI with respect to system parameter and type of stability calculation.**

25	$VCPI_k$	Real time prediction of voltage collapse.	Medium	Online	Low	Load flow parameters.	Steady state /Dynamic
26	$VSLBI_k$	PMU based voltage stability protection.	Medium	Online/ Offline	Low	PMU data	Steady state & also for dynamic load models
27	SG	Determine network sensitivity to voltage collapse.	High	Offline	Low	Load flow data	Steady state

comparison of voltage stability indices based on different qualitative assessment parameters such as their application, accuracy in estimation of voltage stability margin, suitability for online/offline determination of voltage stability, complexity validity under various system parameters, applicability for steady state/transient stability assessment has been presented.

V. RESEARCH GAPS AND FUTURE NEEDS

Most of the research on voltage stability studies has been carried out for transmission networks. Very limited efforts seem to be made in the voltage stability assessment of distribution networks. Smart grid architecture encourages the use of renewable energy resources. These renewable resources may be utilized as distributed generations that are capable of supplying a part of the network locally in a microgrid structure. Modern power system comprises of intermittent generation sources like wind and photovoltaic generation & dynamic loads like EVs and electric motors. These intermittent generation sources and dynamic loads are highly unpredictable, nonlinear in nature. Also, the dynamic response of the such system due to introduction of inverters is different from the conventional power system. These unpredictable, nonlinear and dynamic characteristics are limiting the use of existing voltage stability indices in the current power system composed of intermittent generation sources such as wind and photovoltaic generation. Therefore, conventional voltage stability indices may not be suitable for stability assessment under such circumstances. Further effort is required in this regard. However, the indices presented for static analysis can be utilized to evaluate the power system network integrated with distributed generation and electric vehicles without considering its dynamic behavior. Figure 5 has presented a few indices that may be helpful in the voltage stability assessment of distribution networks. A comprehensive presentation of different indices considering different qualitative aspects are shown in Table 3. It is observed from Table 3 that a very limited number of indices have been suggested in the literature for online assessment of voltage stability. With the advancement in synchro phasor measurement technology, it is quite possible to monitor and control the voltage stability of the system in a real-time framework. Future research must suggest indices that can effectively monitor and control the voltage stability margin of the real-time system through regular update of voltage stability margin. Further the proposed indices may be validated on test systems proposed in [125].

VI. PROPOSED FRAMEWORK FOR SELECTING VSIs

This section discusses the applicability of this comprehensive review article for selection of VSIs. As numerous VSIs are available in the literature, it is very difficult to select suitable VSIs for a given problem. However, this survey with the help of Tables 2 & 3 proposes a framework (Fig. 6), for optimistically shortlisting fewer VSIs for the purpose. The approach has been discussed by considering five popular use cases.

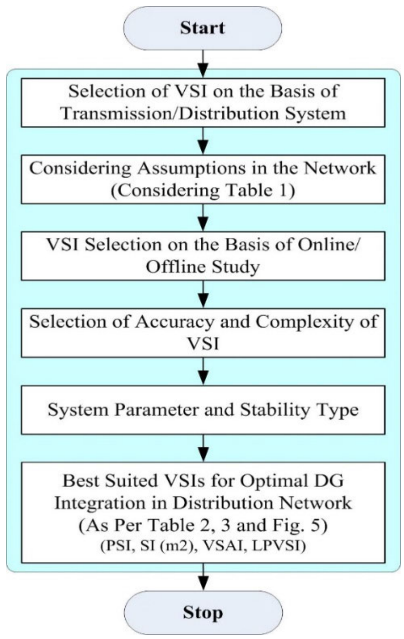

FIGURE 6. **Framework for selecting suitable VSIs for optimal DG integration in radial distribution system.**

Scenario 1: VSI Selection for optimal DG integration in radial distribution system.

Consider an example of selecting a suitable VSI for optimal DG integration in a given radial distribution network. As the problem is related to Distribution network, we can simply omit VSI applicable to transmission systems with the help of Fig. 5. Further, Table 2 may be utilized for further shortlisting of the suitable VSIs. Generally, the weakest bus of the Distribution network is selected for DG placement, thus, VSI, calculating bus stability may be preferred over VSIs quantifying line stability. Further, for the distribution system, the resistance of the branch connecting two buses (i.e., $r_{ij} \neq 0$) must not be neglected. Since the location and sizing of DGs is considered at the planning stage of the distribution system, therefore, it come under offline study voltage stability analysis. Also, at the planning stage, we have sufficient time to find the most accurate solution towards our problem. Hence, we have to select the VSI which gives most accurate solution regardless of its complexity. Loading conditions in the distribution system at the planning stage is considered fixed and static stability analysis is good to calculate the location and allocation of DGs in the distribution network. Considering the above facts, the best-suited VSIs for optimal DG integration in the distribution network as per Table 2, 3 and Fig. 5 are PSI, SI(m_2), VSAI, LP_{VSI}.

Scenario 2: VSI Selection for optimal distribution network reconfiguration.

Similar to the optimal DG integration problem, optimal network reconfiguration problem is also tested over distribution networks. So, from figure 5 VSIs applicable to distribution network may be selected. Radial distribution network contains radiality and buses are connected with the help branches/tie branches. Each branch has a switch so that we can divert the flow of power through a path for which the overall voltage stability of the distribution network may be enhanced. The aim of the problem is to select a suitable VSI that calculates voltage stability of the network for the optimal configuration of the network accurately and efficiently. Since the problem is tested over distribution system, so, the assumption for the resistance of the branches connecting buses ($r_{ij} \neq 0$) may not be neglected during selection of the VSI. Optimal distribution network configuration is selected by opening and closing of switches at the planning stage for fix load condition. Hence, VSIs suitable for offline study may be selected. Although if the load is variable in nature and optimal reconfiguration is done in operation stage, VSIs suitable for online study may be selected. At planning stage, we prefer VSIs which gives more accurate solution regardless of the complexity. Loading conditions in distribution system at planning stage is considered fixed and static stability analysis is good to calculate the optimal network configuration of the distribution network. As per the Table 2, 3 and Fig. 5, PSI, SI(m_2), VSAI, LP_{VSI} are the best suited VSIs for optimal network configuration problem.

Scenario 3: VSI Selection for optimal placement of Electric Vehicle Charging Station (EVCS) in distribution network.

Electric Vehicle Charging Stations (EVCS) are generally installed at the load side. Our loads are generally supplied through radial distribution system. The EVCSs may also be considered as load because they are installed in the distribution system to charge/supply power to the Electric Vehicles (EVs). Since the EV load is increasing day-by-day so their charging stations (i.e. EVCSs) should be installed optimally in the distribution network to reduce the possibility of voltage instability/voltage degression at the buses in the distribution system. Since EVCS is connected to the distribution network so, we may not neglect the resistance of the branches connecting buses ($r_{ij} \neq 0$) during the selection of the VSI. Voltage stability indices used for offline study are best suited for optimal placement of EVCS in distribution systems. Since the location of EVCS will be fixed for the given load condition in the distribution system and it would be decided at the time of planning of the distribution system. So, we have to select the VSI which gives most accurate solution no matter how complex is (i.e neglecting most of the assumptions) it. Now considering the above facts static voltage stability analysis is good to calculate the optimal location of the EVCS in the distribution system with the help of the indices like PSI, SI(m_2), VSAI, LP_{VSI}.

Scenario 4: VSI Selection for Critical Reactive Loading at Single Bus in IEEE 14 bus test system.

Considering an example of VSI selection for critical reactive loading in transmission system. As the problem is related to transmission network, we can simply omit VSI applicable to distribution system with the help of Fig. 5. Based on proposed framework line voltage stability indices are most suitable for finding the critical reactive loading at a bus in transmission system. From Table 2 & 3 by using the proposed framework suitable VSI like FVSI, L_{mn}, L_{qp}, LVSI, LVCI, $_{n}$VSI, VSI_{SCC}, LSJ, ILSJ, NLSI, CSI and ITLTI etc may be utilize for selection of critical reactive loading in transmission system. Among these VSIs FVSI, L_{mn}, L_{qp}, LVSI, LVCI have been selected for analyzing the said problem. By increasing the reactive load at each bus till voltage collapse, the ability of the line indices with high reactive loading has been studied on IEEE 14-bus test system (Figure 7).

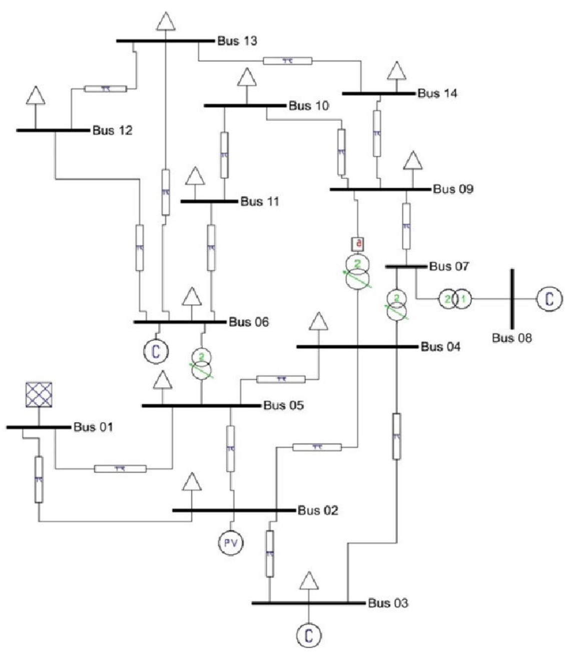

FIGURE 7. IEEE 14-bus test system.

TABLE 4. Line indices for an IEEE 14-bus system with critical reactive loads at a single bus.

Bus No.	Critical Reactive Loading (p.u.)	Lines		Line Stability Indices (in p.u.)					Most Critical Line
		From Bus	To Bus	FVSI	L_{mn}	L_{qp}	LVSI	LVCI	
14	1.191	14	13	1.1108	0.9834	0.8473	1.6007	1.0812	14-13
		9	14	1.0832	0.9763	0.9176	1.7113	1.1540	
		6	13	0.4688	0.7131	0.5688	1.7881	1.7328	
5	5.935	2	5	1.0177	1.0031	1.0101	1.1058	1.0202	2-5
		5	1	0.9173	1.0030	0.7355	0.6464	1.0593	
		5	6	0.9275	0.9876	0.8570	0.0000	1.0356	
4	6.005	2	4	1.0061	1.0032	1.0092	0.9695	1.0161	2-4
		3	4	1.1352	1.0009	1.0756	2.4106	1.2364	
		4	7	0.8887	0.9029	0.8620	0.0000	1.3796	
10	1.812	11	10	0.9657	0.9030	0.8341	1.7234	1.3114	11-10
		9	10	0.8525	0.8022	0.7490	1.9945	1.4448	
		6	11	0.8396	0.8018	0.7037	0.0000	1.4452	
13	2.871	6	13	1.1805	0.9877	0.9855	1.9252	1.0025	6-13
		12	13	1.4542	0.9776	0.6852	1.8087	1.1496	
		14	13	0.9115	0.8313	0.7411	1.9065	1.4107	
12	1.765	12	13	1.5592	1.0001	2.5378	1.7144	1.0109	12-13
		6	12	1.1828	0.9885	1.0909	2.3365	1.0208	
		6	13	0.9875	0.9826	0.8163	1.6409	1.6612	
11	1.941	6	11	1.1539	0.9885	0.9865	1.8335	1.0015	6-11
		9	10	0.4475	0.4408	0.3941	1.8646	1.7478	
		8	7	0.4195	0.4195	0.4195	1.7619	1.7619	
9	2.484	4	9	1.0488	1.0638	1.0502	0.0000	1.1627	4-9
		7	9	0.8759	0.8788	0.8819	0.0000	1.3481	
		11	10	0.8189	0.7915	0.7107	1.6462	1.4566	

TABLE 5. Line indices for the most critical lines in the IEEE 14-bus system under critical contingencies with critical MVA loadings.

Critical Line Outage	Maximum MVA Loading (p.u.)	Most Critical Line	Line Stability Indices (in p.u.)				
			FVSI	L_{mn}	L_{qp}	LVSI	LVCI
6-13	3.220	14-13	1.0894	1.0812	1.1055	1.1245	1.0154
3-2	2.261	2-4	1.1252	1.0238	2.0231	1.2254	1.0541
1-2	1.336	1-5	0.7945	0.7983	1.4324	1.1145	1.0242
7-9	2.883	4-9	1.0825	1.1580	1.0622	0.0000	1.0011
5-6	2.279	1-5	1.0621	1.0401	1.026	1.1899	1.0024

For critical reactive loading at a single bus, the values of the LVCI index and LVSI should be very near to 2, while the values of L_{mn}, FVSI, and L_{qp} should be very close to 1. The line indices value at a single bus under heavy loading is shown in Table 4. When there is high reactive loading at bus number 4, the values of the line indices other than the LVCI index exceed their critical limits. However, the LVCI index value for the (2)-(4) is 1.0161 p.u., which is very close to 1 but not less than or equal to unity, indicating high accuracy in the voltage stability prediction. As a result, other indices cannot reliably forecast the voltage stability in this situation. It is feasible to determine the system's critical line in this case with accuracy as line (2)-(4). Similarly, the lines indicated in the last column of Table 4 are the most stressed lines in the system when there is significant reactive loading at a single bus. The most critical line indices, L_{mn}, FVSI, and L_{qp}, are found to be 1.0638 p.u., 1.0488 p.u., and 1.0502 p.u., respectively, in the case of heavy reactive loading at bus 9. This indicates that the system is under voltage collapse condition, while the LVSI index value is zero, indicating the failure of the voltage stability prediction. The LVCI index value in this instance drops to 1.1627 p.u., indicating that lines (4)–(9) are stressed and require for the necessary control measures.

Scenario 5: N-1 Contingency Analysis under Heavy MVA Loading in IEEE 14 bus test system.

Similar to the VSI selection for critical reactive loading problem N-1 contingency analysis under heavy MVA loading is also tested over transmission system. Voltage stability indices best suitable for transmission network may be selected from Fig. 5. Further VSIs suitable for line stability assessment for N-1 contingency analysis under heavy MVA loading may be selected from Table 2 and 3 by using the proposed framework. By using the proposed framework FVSI, L_{mn}, L_{qp}, LVSI, LVCI are few VSIs selected here for N-1 contingency analysis under heavy MVA loading. In terms of contingencies, the most severe one is the one with the lowest maximum MVA loading. For the voltage stability analysis under high MVA loading scenarios, the top five severe contingencies are taken into account in IEEE 14-bus test system. These extreme scenarios include line outages (6)-(13), (3)-(2), (1)-(2), (7)-(9), and (5)-(6), The most stressed lines under these severe contingencies are (14)-(13), (2)-(4), (1)-(5), (4)-(9), and (1)-(5), respectively. Under the maximum allowable MVA loading, the line index values of Lmn, FVSI, and Lqp should be equal to or less than unity. The indices LVCI and LVSI in this case should have values that are larger than or equal to unity. Table 5 indicates that the Lmn, FVSI, and Lqp values of the most stressed lines are either greater than or significantly less than unity (not close to unity) under severe contingency conditions. This indicates that these indices are not suitable for measuring voltage stability (line severity). On the other hand, the LVSI values of the majority of severe lines are greater than or distant from unity. However, in severe contingencies cases, the LVCI index values are greater than or almost equal to unity, demonstrating the excellent precision and usefulness of this index in determining the system's voltage stability as measured by the line stability index.

VII. CONCLUSION

An elaborative investigation that delineates several VSIs proposed in works over the past few decades has been presented in the paper. This work delivers an exhaustive elucidation of the VSIs concepts, derivation, critical values, assumptions for obtaining indices, efficacy and pertinence in terms of their merits and demerits. These VSIs can be applied to find absolute/relative stability of any network and can be calculated online or offline. To calculate these indices, we need to know P, Q, V, δ and line parameters. The correctness of any VSI in calculating the stability thus depends on the precision of the instruments measuring these quantities. In addition, accuracy also depends on the number of assumptions undertaken while deriving the VSIs. Thus, it is necessary to understand the intricacies of the VSIs before selecting a suitable one for a given problem. Henceforth, this work makes extensive knowledge addition and can be considered as a means of information for investigators, academicians, and power engineers in context of voltage instability prediction and prevention, DG placing and rating, voltage stability assessment, power system planning and other related fields. Further research is required to suggest new indices that are applicable in a smart grid architecture for real-time monitoring and control of voltage stability margin.

ACKNOWLEDGMENT

The authors extend their appreciation to the Researchers Supporting Project at King Saud University, Riyadh, Saudi Arabia, for funding this research work through the project number RSP-2021/278. The authors would like to acknowledge the support from Intelligent Prognostic Private Limited Delhi, India for providing support for carrying out this research work. The authors extend their appreciation to the Researchers Supporting Project at Universiti Teknologi Malaysia (UTM), Malaysia (project no. UTMFR: Q.J130000.3823.23H05).

REFERENCES

[1] O. Alizadeh Mousavi, M. Bozorg, and R. Cherkaoui, "Preventive reactive power management for improving voltage stability margin," *Electric Power Syst. Res.*, vol. 96, pp. 36–46, Mar. 2013.

[2] P. S. Kundur, *Power System Stability and Control*, vol. 1. New York, NY, USA: McGraw-Hill, 2004, pp. 1–600.

[3] M. Eremia and M. Shahidehpour, *Handbook of Electrical Power System Dynamics: Modeling, Stability, and Control*, vol. 92. Hoboken, NJ, USA: Wiley, 2013.

[4] M. Kamel, A. A. Karrar, and A. H. Eltom, "Development and application of a new voltage stability index for on-line monitoring and shedding," *IEEE Trans. Power Syst.*, vol. 33, no. 2, pp. 1231–1241, Mar. 2018, doi: 10.1109/TPWRS.2017.2722984.

[5] C. D. Vournas, C. Lambrou, and P. Mandoulidis, "Voltage stability monitoring from a transmission bus PMU," *IEEE Trans. Power Syst.*, vol. 32, no. 4, pp. 3266–3274, Jul. 2017, doi: 10.1109/TPWRS.2016.2629495.

[6] L. Huang, J. Xu, Y. Sun, T. Cui, and F. Dai, "Online monitoring of wide-area voltage stability based on short circuit capacity," in *Proc. Asia–Pacific Power Energy Eng. Conf.*, Mar. 2011, pp. 1–5, doi: 10.1109/APPEEC.2011.5747730.

[7] H. Tanaka, K. Tokumitsu, S. Iwamoto, R. Kobayashi, D. Hirano, and A. Takeuchi, "Development of the emergency voltage control scheme using VMPI," in *Proc. IEEE Power Energy Soc. Gen. Meeting*, Jul. 2009, pp. 1–6, doi: 10.1109/PES.2009.5275513.

[8] S. K., S. N. Singh, and S. C. Srivastava, "A synchrophasor assisted frequency and voltage stability based load shedding scheme for self-healing of power system," *IEEE Trans. Smart Grid*, vol. 2, no. 2, pp. 221–230, Jun. 2011, doi: 10.1109/TSG.2011.2113361.

[9] K. T. Vu, D. Julian, abd J. Gjerde, "Application and methods for voltage stability pridiction," U.S. Patent 6 249 719, 2001.

[10] L. J. S. Damião, W. G. Zvietcovich, and F. R. A. C. Baracho, "Optimal reconfiguration of power distribution network for stability voltage and power quality improvements," in *Proc. Int. Conf. Smart Grid (icSmartGrid)*, Dec. 2018, pp. 82–87, doi: 10.1109/ISGWCP.2018.8634463.

[11] R. D. de Moura and R. B. Prada, "Contingency screening and ranking method for voltage stability assessment," *IEE Proc. Gener., Transmiss. Distribution*, vol. 152, no. 6, p. 891, 2005, doi: 10.1049/ip-gtd:20045289.

[12] M. Parniani and M. Vanouni, "A fast local index for online estimation of closeness to loadability limit," *IEEE Trans. Power Syst.*, vol. 25, no. 1, pp. 584–585, Feb. 2010, doi: 10.1109/TPWRS.2009.2036460.

[13] A. Mishra and G. V. N. Kumar, "A risk of severity based scheme for optimal placement of interline power flow controller using composite index," *Int. J. Power Energy Convers.*, vol. 8, no. 3, p. 257, 2017, doi: 10.1504/ijpec.2017.084911.

[14] S. Fang, S. Member, H. Cheng, and Y. Song, "A new type of MW and MVar dispatch index for meeting voltage stability margin criteria based on normal vector of limit surface," in *Proc. IEEE Power Energy Soc. Gen. Meeting*, Jul. 2015, vol. 4, no. 2, pp. 1–7, doi: 10.1109/PESGM.2015.7285814.

[15] W. Gu and Q. Wan, "Linearized voltage stability index for wide-area voltage monitoring and control," *Int. J. Electr. Power Energy Syst.*, vol. 32, no. 4, pp. 333–336, May 2010, doi: 10.1016/j.ijepes.2009.09.003.

[16] M. Glavic and T. Van Cutsem, "Wide-area detection of voltage instability from synchronized phasor measurements. Part I: Principle," *IEEE Trans. Power Syst.*, vol. 24, no. 3, pp. 1408–1416, Aug. 2009.

[17] S. Kamel, M. Mohamed, A. Selim, L. S. Nasrat, and F. Jurado, "Power system voltage stability based on optimal size and location of shunt capacitor using analytical technique," in *Proc. 10th Int. Renew. Energy Congr. (IREC)*, Mar. 2019, pp. 1–5, doi: 10.1109/IREC.2019.8754516.

[18] M. E. C. Bento, "Physics-guided neural network for load margin assessment of power systems," *IEEE Trans. Power Syst.*, vol. 39, no. 1, pp. 564–575, Jan. 2024, doi: 10.1109/TPWRS.2023.3266236.

[19] M. Ghafouri, M. Au, M. Kassouf, M. Debbabi, C. Assi, and J. Yan, "Detection and mitigation of cyber attacks on voltage stability monitoring of smart grids," *IEEE Trans. Smart Grid*, vol. 11, no. 6, pp. 5227–5238, Nov. 2020, doi: 10.1109/TSG.2020.3004303.

[20] R. Viral and D. K. Khatod, "Optimal planning of distributed generation systems in distribution system: A review," *Renew. Sustain. Energy Rev.*, vol. 16, no. 7, pp. 5146–5165, Sep. 2012, doi: 10.1016/j.rser.2012.05.020.

[21] R. Viral and D. K. Khatod, "An analytical approach for sizing and siting of DGs in balanced radial distribution networks for loss minimization," *Int. J. Electr. Power Energy Syst.*, vol. 67, pp. 191–201, May 2015, doi: 10.1016/j.ijepes.2014.11.017.

[22] T. Ackermann, G. Andersson, and L. Söder, "Distributed generation: A definition," *Electric Power Syst. Res.*, vol. 57, no. 3, pp. 195–204, Apr. 2001, doi: 10.1016/s0378-7796(01)00101-8.

[23] G. Pepermans, J. Driesen, D. Haeseldonckx, R. Belmans, and W. D'haeseleer, "Distributed generation: Definition, benefits and issues," *Energy Policy*, vol. 33, no. 6, pp. 787–798, Apr. 2005, doi: 10.1016/j.enpol.2003.10.004.

[24] M. S. S. Danish, T. Senjyu, S. M. S. Danish, N. R. Sabory, N. K, and P. Mandal, "A recap of voltage stability indices in the past three decades," *Energies*, vol. 12, no. 8, p. 1544, Apr. 2019, doi: 10.3390/en12081544.

[25] J. Modarresi, E. Gholipour, and A. Khodabakhshian, "A comprehensive review of the voltage stability indices," *Renew. Sustain. Energy Rev.*, vol. 63, pp. 1–12, Sep. 2016, doi: 10.1016/j.rser.2016.05.010.

[26] A. Nageswa Rao, P. Vijaya, and M. Kowsalya, "Voltage stability indices for stability assessment: A review," *Int. J. Ambient Energy*, vol. 42, no. 7, pp. 829–845, May 2021, doi: 10.1080/01430750.2018.1525585.

[27] H. Zaheb, M. S. S. Danish, T. Senjyu, M. Ahmadi, A. M. Nazari, M. Wali, M. Khosravy, and P. Mandal, "A contemporary novel classification of voltage stability indices," *Appl. Sci.*, vol. 10, no. 5, p. 1639, Feb. 2020, doi: 10.3390/app10051639.

[28] P. Kundur, J. Paserba, V. Ajjarapu, G. Andersson, and A. Bose, "Definition and classification of power system stability IEEE/CIGRE joint task force on stability terms and definitions," *IEEE Trans. Power Syst.*, vol. 19, no. 2, pp. 1387–1401, Aug. 2004, doi: 10.1109/TPWRS.2004.825981.

[29] N. Hatziargyriou, J. Milanovic, C. Rahmann, V. Ajjarapu, C. Canizares, I. Erlich, D. Hill, I. Hiskens, I. Kamwa, B. Pal, P. Pourbeik, J. Sanchez-Gasca, A. Stankovic, T. Van Cutsem, V. Vittal, and C. Vournas, "Definition and classification of power system stability–revisited & extended," *IEEE Trans. Power Syst.*, vol. 36, no. 4, pp. 3271–3281, Jul. 2021, doi: 10.1109/TPWRS.2020.3041774.

[30] N. J. F. Kiessling and P. Neffzger, *Overhead Power Lines—Planning, Design, Construction*. Berlin, Germany: Springer, 2003.

[31] D. Q. Hung, N. Mithulananthan, and R. C. Bansal, "Analytical expressions for DG allocation in primary distribution networks," *IEEE Trans. Energy Convers.*, vol. 25, no. 3, pp. 814–820, Sep. 2010, doi: 10.1109/TEC.2010.2044414.

[32] J. John, J. Grainger, and W. D. Stevenson, *Power System Analysis* (Series in Electrical and Computer Engineering), 4th ed., Singapore: McGraw-Hill, 1994.

[33] M. M. Aman, G. B. Jasmon, H. Mokhlis, and A. H. A. Bakar, "Optimal placement and sizing of a DG based on a new power stability index and line losses," *Int. J. Electr. Power Energy Syst.*, vol. 43, no. 1, pp. 1296–1304, Dec. 2012, doi: 10.1016/j.ijepes.2012.05.053.

[34] A. R. Bergen and V. Vittal, *Power Systems Analysis*, 2nd ed., London, U.K.: Pearson, 2000.

[35] M. Moghavvemi and O. Faruque, "Real-time contingency evaluation and ranking technique," *IEE Proc. Gener., Transmiss. Distribution*, vol. 145, no. 5, p. 517, 1998, doi: 10.1049/ip-gtd:19982179.

[36] Z. J. Lim, M. W. Mustafa, and Z. B. Muda, "Evaluation of the effectiveness of voltage stability indices on different loadings," in *Proc. IEEE Int. Power Eng. Optim. Conf. (PEOCO)*, Jun. 2012, pp. 543–547, doi: 10.1109/PEOCO.2012.6230925.

[37] I. Musirin and T. K. A. Rahman, "Estimating maximum loadability for weak bus identification using FVSI," *IEEE Power Eng. Rev.*, vol. 22, no. 11, pp. 50–52, Nov. 2002, doi: 10.1109/MPER.2002.4311799.

[38] I. Musirin and T. K. A. Rahman, "Novel fast voltage stability index (FVSI) for voltage stability analysis in power transmission system," in *Proc. Student Conf. Res. Develop.*, Jul. 2002, pp. 265–268, doi: 10.1109/SCORED.2002.1033108.

[39] R. Kanimozhi and K. Selvi, "A novel line stability index for voltage stability analysis and contingency ranking in power system using fuzzy based load flow," *J. Electr. Eng. Technol.*, vol. 8, no. 4, pp. 694–703, Jul. 2013, doi: 10.5370/JEET.2013.8.4.694.

[40] A. Mohamed, G. B. Jasmon, and S. Yusof, "A static voltage collapse indicator using line stability factors," *J. Ind. Technol.*, vol. 7, no. 1, pp. 73–85, 1989.

[41] M. Moghavvemi and M. O. Faruque, "Technique for assessment of voltage stability in ill-conditioned radial distribution network," *IEEE Power Eng. Rev.*, vol. 21, no. 1, pp. 58–60, Jul. 2001, doi: 10.1109/39.893345.

[42] A. Yazdanpanah-Goharrizi and R. Asghari, "A novel line stability index (NLSI) for voltage stability assessment of power systems," in *Proc. 7th WSEAS*, 2007, pp. 164–167.

[43] F. A. Althowibi and M. W. Mustafa, "Line voltage stability calculations in power systems," in *Proc. IEEE Int. Conf. Power Energy*. Malaysia: IEEE, Nov. 2010, pp. 396–401, doi: 10.1109/PECON.2010.5697616.

[44] T. K. A. Rahman and G. B. Jasmon, "A new technique for voltage stability analysis in a power system and improved loadflow algorithm for distribution network," in *Proc. Int. Conf. Energy Manage. Power Del. EMPD*. Singapore: IEEE, Sep. 1995, pp. 714–719, doi: 10.1109/EMPD.1995.500816.

[45] V. G. K. Makasa and K. Joseph, "On-line voltage stability load index estimation based on PMU measurements," in *Proc. IEEE Power and Energy Society General Meeting*. Detroit, MI, USA: IEEE, 2011, pp. 1–6, doi: 10.1109/PES.2011.6039882.

[46] S. Sahari, A. F. Abidin, and T. K. Abdul Rahman, "Development of artificial neural network for voltage stability monitoring," in *Proc. Nat. Power Eng. Conf. (PECon)*, 2003, pp. 37–42, doi: 10.1109/pecon.2003.1437413.

[47] T. K. Chattopadhyay, S. Banerjee, and C. K. Chanda, "Impact of distributed generator on voltage stability analysis of distribution networks under critical loading conditions," in *Proc. 1st Int. Conf. Non Conventional Energy (ICONCE)*. India: IEEE, Jan. 2014, pp. 288–291, doi: 10.1109/ICONCE.2014.6808728.

[48] U. Eminoglu and M. H. Hocaoglu, "A voltage stability index for radial distribution networks," in *Proc. 42nd Int. Universities Power Eng. Conf.*, Brighton, U.K., Sep. 2007, pp. 408–413, doi: 10.1109/UPEC.2007.4468982.

[49] R. Tiwari, K. R. Niazi, and V. Gupta, "Line collapse proximity index for prediction of voltage collapse in power systems," *Int. J. Electr. Power Energy Syst.*, vol. 41, no. 1, pp. 105–111, Oct. 2012, doi: 10.1016/j.ijepes.2012.03.022.

[50] A. M. Chebbo, M. R. Irving, and M. J. H. Sterling, "Voltage collapse proximity indicator: Behaviour and implications," Barcelona, Spain: IEEE, 1992, pp. 241–252, doi: 10.1109/EPQU.2007.4424089.

[51] M. A. Albuquerque and C. A. Castro, "A contingency ranking method for voltage stability in real time operation of power systems," in *Proc. IEEE Bologna Power Tech Conf.*, Sep. 2003, pp. 490–494, doi: 10.1109/PTC.2003.1304177.

[52] M. Nizam, A. Mohamed, M. Al-Dabbagh, and A. Hussain, "Dynamic voltage collapse prediction in a practical power system with support vector machine," in *Proc. TENCON IEEE Region 10 Conf.* India: IEEE, Nov. 2008, pp. 777–780, doi: 10.1109/TENCON.2008.4766855.

[53] Y. Gong and N. Schulz, "Synchrophasor-based real-time voltage stability index," in *Proc. IEEE PES Power Syst. Conf. Exposit.*, Oct. 2006, pp. 1029–1036, doi: 10.1109/PSCE.2006.296452.

[54] G. Deng, Y. Sun, and J. Xu, "A new index of voltage stability considering distribution network," in *Proc. Asia–Pacific Power Energy Eng. Conf. (APPEEC)*, 2009, pp. 1–4, doi: 10.1109/APPEEC.2009.4918070.

[55] T. He, S. Kolluri, S. Mandal, F. Galvan, and P. Rasigoufard, "Identification of weak locations in bulk transmission systems using voltage stability margin index," in *Proc. IEEE Power Eng. Soc. Gen. Meeting*. Denver, CO, USA: IEEE, Aug. 2004, pp. 1814–1819, doi: 10.1109/PES.2004.1373193.

[56] K. Vu, M. M. Begouic, and D. Novosel, "Grids get smart protection and control," *IEEE Comput. Appl. Power*, vol. 10, no. 4, pp. 40–44, Oct. 1997, doi: 10.1109/67.625373.

[57] A. Wiszniewski, "New criteria of voltage stability margin for the purpose of load shedding," *IEEE Trans. Power Del.*, vol. 22, no. 3, pp. 1367–1371, Jul. 2007, doi: 10.1109/TPWRD.2006.886772.

[58] G. Yesuratnam and D. Thukaram, "Congestion management in open access based on relative electrical distances using voltage stability criteria," *Electric Power Syst. Res.*, vol. 77, no. 12, pp. 1608–1618, Oct. 2007, doi: 10.1016/j.epsr.2006.11.007.

[59] B. Genêt and J.-C. Maun, "Voltage-stability monitoring using wide-area measurement systems," in *Proc. IEEE Lausanne Power Tech.*, Jul. 2007, pp. 1712–1717, doi: 10.1109/PCT.2007.4538573.

[60] S. Pérez-Londoño, L. F. Rodríguez, and G. Olivar, "A simplified voltage stability index (SVSI)," *Int. J. Electr. Power Energy Syst.*, vol. 63, pp. 806–813, Dec. 2014, doi: 10.1016/j.ijepes.2014.06.044.

[61] I. Smon, G. Verbic, and F. Gubina, "Local voltage-stability index using Tellegen's theorem," *IEEE Trans. Power Syst.*, vol. 21, no. 3, pp. 1267–1275, Aug. 2006, doi: 10.1109/TPWRS.2006.876702.

[62] C. W. Taylor, *Power System Voltage Stability*, 2nd ed., New York, NY, USA: McGraw-Hill, 1994.

[63] M. H. Haque, "Use of local information to determine the distance to voltage collapse," *Int. J. Emerg. Electric Power Syst.*, vol. 9, no. 2, pp. 1–14, Mar. 2008, doi: 10.2202/1553-779x.1911.

[64] G. Verbic and F. Gubina, "A new concept of protection against voltage collapse based on local phasors," in *Proc. PowerCon. Int. Conf. Power Syst. Technol.*, 2000, vol. 2, no. 2, pp. 965–970, doi: 10.1109/icpst.2000.897151.

[65] V. Balamourougan, T. S. Sidhu, and M. S. Sachdev, "Technique for online prediction of voltage collapse," *IEE Proc. Gener., Transmiss. Distribution*, vol. 151, no. 4, p. 453, 2004, doi: 10.1049/ip-gtd:20040612.

[66] B. Milosevic and M. Begovic, "Voltage-stability protection and control using a wide-area network of phasor measurements," *IEEE Trans. Power Syst.*, vol. 18, no. 1, pp. 121–127, Feb. 2003, doi: 10.1109/TPWRS.2002.805018.

[67] F. A. Althowibi and M. W. Mustafa, "Power system network sensitivity to voltage collapse," in *Proc. IEEE Int. Power Eng. Optim. Conf.*, Jun. 2012, pp. 379–383, doi: 10.1109/PEOCO.2012.6230893.

[68] M. C. Gutzwiller, *Interdisciplinary Applied Mathematics*, vol. 5. Berlin, Germany: Springer-Varlag, 1990.

[69] A. C. Z. de Souza, C. A. Canizares, and V. H. Quintana, "New techniques to speed up voltage collapse computations using tangent vectors," *IEEE Trans. Power Syst.*, vol. 12, no. 3, pp. 1380–1387, Sep. 1997, doi: 10.1109/59.630485.

[70] A. C. Z. de Souza, "Discussion on some voltage collapse indices," *Electric Power Syst. Res.*, vol. 53, no. 1, pp. 53–58, Jan. 2000, doi: 10.1016/s0378-7796(99)00042-5.

[71] C. De Marco and A. Bergen, "A security measure for random load disturbances in nonlinear power system models," *IEEE Trans. Circuits Syst.*, vol. CS-34, no. 12, pp. 1546–1557, Dec. 1987, doi: 10.1109/TCS.1987.1086092.

[72] C. L. DeMarco and T. J. Overbye, "An energy based security measure for assessing vulnerability to voltage collapse," *IEEE Trans. Power Syst.*, vol. 5, no. 2, pp. 419–427, May 1990, doi: 10.1109/59.54548.

[73] E. V. De Lorenci, A. C. Z. de Souza, and B. I. L. Lopes, "Energy function applied to voltage stability studies–discussion on low voltage solutions with the help of tangent vector," *Electric Power Syst. Res.*, vol. 141, pp. 290–299, Dec. 2016, doi: 10.1016/j.epsr.2016.08.004.

[74] T. J. Overbye and C. L. De Marco, "Voltage security enhancement using energy based sensitivities," *IEEE Trans. Power Syst.*, vol. 6, no. 3, pp. 1196–1202, Dec. 1991, doi: 10.1109/59.119266.

[75] A. C. Z. de Souza, R. C. Leme, L. F. B. Vasconcelos, B. I. L. Lopes, and Y. C. da Silva Ribeiro, "Energy function and unstable solutions by the means of an augmented Jacobian," *Appl. Math. Comput.*, vol. 206, no. 1, pp. 154–163, Dec. 2008, doi: 10.1016/j.amc.2008.08.040.

[76] B. Gao, G. K. Morison, and P. Kundur, "Voltage stability evaluation using modal analysis," *IEEE Trans. Power Syst.*, vol. 7, no. 4, pp. 1529–1542, May 1992, doi: 10.1109/59.207377.

[77] M. Moghavvemi and F. M. Omar, "Technique for contingency monitoring and voltage collapse prediction," *IEE Proc. Gener., Transmiss. Distribution*, vol. 145, no. 6, p. 634, 1998, doi: 10.1049/ip-gtd:19982355.

[78] B. Ismail, N. I. A. Wahab, M. L. Othman, M. A. M. Radzi, K. N. Vijyakumar, and M. N. Mat Naain, "A comprehensive review on optimal location and sizing of reactive power compensation using hybrid-based approaches for power loss reduction, voltage stability improvement, voltage profile enhancement and loadability enhancement," *IEEE Access*, vol. 8, pp. 222733–222765, 2020, doi: 10.1109/ACCESS.2020.3043297.

[79] C. Subramani, S. S. Dash, M. A. Bhaskar, M. Jagadeeshkumar, K. Sureshkumar, and R. Parthipan, "Line outage contingency screening and ranking for voltage stability assessment," in *Proc. Int. Conf. Power Syst.*, Dec. 2009, pp. 1–5, doi: 10.1109/ICPWS.2009.5442743.

[80] M. K. Meena and N. Kumar, "On-line monitoring and simulation of transmission line network voltage stability using FVSI," in *Proc. 2nd IEEE Int. Conf. Power Electron., Intell. Control Energy Syst. (ICPEICES)*, Oct. 2018, pp. 257–260, doi: 10.1109/ICPEICES.2018.8897403.

[81] T. Subramaniam, M. S. Abd Rahman, A. M. Ariffin, and M. Sahrim, "An investigation on the power system stability of photovoltaic grid integrated system," in *Proc. 7th IEEE Int. Conf. Control Syst., Comput. Eng. (ICCSCE)*, Nov. 2017, pp. 356–359, doi: 10.1109/ICCSCE.2017.8284434.

[82] I. A. Araga and A. E. Airoboman, "Enhancement of voltage stability in an interconnected network using unified power flow controller," *J. Adv. Sci. Eng.*, vol. 4, no. 1, pp. 65–74, Jan. 2021, doi: 10.37121/jase.v4i1.141.

[83] M. Furukakoi, O. B. Adewuyi, M. S. S. Danish, A. M. Howlader, T. Senjyu, and T. Funabashi, "Critical boundary index (CBI) based on active and reactive power deviations," *Int. J. Electr. Power Energy Syst.*, vol. 100, pp. 50–57, Sep. 2018, doi: 10.1016/j.ijepes.2018.02.010.

[84] M. Usama, H. K. Mohamed, I. A. M. El-Maddah, and M. A. Shedied, "A smart voltage stability maneuver algorithm for voltage collapses mitigation," in *Proc. 12th Int. Conf. Comput. Eng. Syst. (ICCES)*. Egypt: IEEE, Dec. 2017, pp. 533–539, doi: 10.1109/ICCES.2017.8275365.

[85] P. Rastgoufard and J. Bian, "Voltage stability study for entergy services," Entergy Services Ltd., Entergy Building, New Orleans, LA, USA, Tech. Rep., 1993.

[86] R. Seydel, *Practical Bifurcation and Stability Analysis*, vol. 5. Berlin, Germany: Springer, 2009.

[87] P. Kessel and H. Glavitsch, "Estimating the voltage stability of a power system," *IEEE Trans. Power Del.*, vol. PD-1, no. 3, pp. 346–354, Sep. 1986, doi: 10.1109/TPWRD.1986.4308013.

[88] M. Chakravorty and D. Das, "Voltage stability analysis of radial distribution networks," *Int. J. Electr. Power Energy Syst.*, vol. 23, no. 2, pp. 129–135, Feb. 2001, doi: 10.1016/s0142-0615(00)00040-5.

[89] Y. Wang, W. Li, and J. Lu, "A new node voltage stability index based on local voltage phasors," *Electric Power Syst. Res.*, vol. 79, no. 1, pp. 265–271, Jan. 2009, doi: 10.1016/j.epsr.2008.06.010.

[90] P. Kayal and C. K. Chanda, "Placement of wind and solar based DGs in distribution system for power loss minimization and voltage stability improvement," *Int. J. Electr. Power Energy Syst.*, vol. 53, pp. 795–809, Dec. 2013, doi: 10.1016/j.ijepes.2013.05.047.

[91] S. Ratra, R. Tiwari, and K. R. Niazi, "Voltage stability assessment in power systems using line voltage stability index," *Comput. Electr. Eng.*, vol. 70, pp. 199–211, Aug. 2018, doi: 10.1016/j.compeleceng.2017.12.046.

[92] S.-J. Chuang, C.-M. Hong, and C.-H. Chen, "Improvement of integrated transmission line transfer index for power system voltage stability," *Int. J. Electr. Power Energy Syst.*, vol. 78, pp. 830–836, Jun. 2016, doi: 10.1016/j.ijepes.2015.11.111.

[93] L. Wang, Y. Liu, and Z. Luan, "Power transmission paths based voltage stability assessment," in *Proc. IEEE/PES Transmiss. Distribution Conf. Expo. Asia–Pacific*, 2005, pp. 1–5, doi: 10.1109/TDC.2005.1546950.

[94] Y. Venu and S. kanthala, "Optimal placement and sizing of compensator for voltage stability improvement using voltage collapse proximity indicator," in *Proc. 3rd Int. Conf. Electron., Commun. Aerosp. Technol. (ICECA)*, Jun. 2019, pp. 690–695, doi: 10.1109/ICECA.2019.8822017.

[95] H. Chen, T. Jiang, H. Yuan, H. Jia, L. Bai, and F. Li, "Wide-area measurement-based voltage stability sensitivity and its application in voltage control," *Int. J. Electr. Power Energy Syst.*, vol. 88, pp. 87–98, Jun. 2017, doi: 10.1016/j.ijepes.2016.12.011.

[96] A. R. R. Matavalam and V. Ajjarapu, "Calculating the long term voltage stability margin using a linear index," in *Proc. IEEE Power Energy Soc. Gen. Meeting*, Jul. 2015, pp. 1–5, doi: 10.1109/PESGM.2015.7285952.

[97] Y. Song, D. J. Hill, and T. Liu, "Static voltage stability analysis of distribution systems based on network-load admittance ratio," *IEEE Trans. Power Syst.*, vol. 34, no. 3, pp. 2270–2280, May 2019, doi: 10.1109/TPWRS.2018.2886636.

[98] A. K. Sinha and D. Hazarika, "A comparative study of voltage stability indices in a power system," *Int. J. Electr. Power Energy Syst.*, vol. 22, no. 8, pp. 589–596, Nov. 2000, doi: 10.1016/s0142-0615(00)00014-4.

[99] M. V. Suganyadevia and C. K. Babulalb, "Estimating of loadability margin of a power system by comparing voltage stability indices," in *Proc. Int. Conf. Control, Autom., Commun. Energy Conservation*, Jun. 2009, pp. 1–4.

[100] A. Rath, S. R. Ghatak, and P. Goyal, "Optimal allocation of distributed generation (DGs) and static VAR compensator (SVC) in a power system using revamp voltage stability indicator," in *Proc. Nat. Power Syst. Conf. (NPSC)*, Dec. 2016, pp. 1–6, doi: 10.1109/NPSC.2016.7858877.

[101] A. Singh, S. R. Ghatak, and S. Dey, "Strategic deployment of distributed generation and DSTATCOM in radial distribution system considering reliability aspect," in *Proc. 2nd Int. Conf. Electron., Mater. Eng. Nano-Technology (IEMENTech)*, May 2018, pp. 1–6, doi: 10.1109/IEMENTECH.2018.8465290.

[102] A. Mishra, V. N. K. Gundavarapu, V. R. Bathina, and D. C. Duvvada, "Real power performance index and line stability index-based management of contingency using firefly algorithm," *IET Gener., Transmiss. Distribution*, vol. 10, no. 10, pp. 2327–2335, Jul. 2016, doi: 10.1049/iet-gtd.2015.1001.

[103] A. Mishra and G. V. N. Kumar, "Severity based contingency management approach: An Indian scenario," *J. Eng. Sci. Technol.*, vol. 12, no. 7, pp. 1833–1844, 2017.

[104] T. Moger and T. Dhadbanjan, "A novel index for identification of weak nodes for reactive compensation to improve voltage stability," *IET Gener., Transmiss. Distribution*, vol. 9, no. 14, pp. 1826–1834, Nov. 2015, doi: 10.1049/iet-gtd.2015.0054.

[105] T. D. T. Moger, "Reactive power loss index for identification of weak nodes and reactive compensation analysis to improve steady state voltage stability," in *Novel Advancements in Electrical Power Planning and Performance*. Hershey, PA, USA: IGI Global, 2020, pp. 177–237, doi: 10.4018/978-1-5225-8551-0.ch007.

[106] S. Konar, D. Chatterjee, and S. Patra, "V–Q sensitivity-based index for assessment of dynamic voltage stability of power systems," *IET Gener., Transmiss. Distribution*, vol. 9, no. 7, pp. 677–685, Apr. 2015, doi: 10.1049/iet-gtd.2014.0710.

[107] X. Ancheng, L. Ruihuang, L. Mingkai, J. H. Chow, B. Tianshu, Y. Ting, and P. Tianjiao, "On-line voltage stability index based on the voltage equation of transmission lines," *IET Gener., Transmiss. Distribution*, vol. 10, no. 14, pp. 3441–3448, Nov. 2016, doi: 10.1049/iet-gtd.2015.1544.

[108] W. Zhao, "A short-term voltage stability index and case studies," *IET Gener. Transmiss. Distrib.*, vol. 2, no. 19, pp. 1–7, Aug. 2017.

[109] T. Nagao, K. Tanaka, and K. Takenaka, "Development of static and simulation programs for voltage stability studies of bulk power system," *IEEE Trans. Power Syst.*, vol. 12, no. 1, pp. 273–281, 1997, doi: 10.1109/59.574948.

[110] J. W. Simpson-Porco and F. Bullo, "Distributed monitoring of voltage collapse sensitivity indices," *IEEE Trans. Smart Grid*, vol. 7, no. 4, pp. 1979–1988, Jul. 2016, doi: 10.1109/TSG.2016.2533319.

[111] F. Gubina and B. Strmcnik, "Voltage collapse proximity index determination using voltage phasors approach," *IEEE Trans. Power Syst.*, vol. 10, no. 2, pp. 788–794, May 1995, doi: 10.1109/59.387918.

[112] I. A. Samuel, J. Katende, C. O. A. Awosope, and A. A. Awelewa, "Prediction of voltage collapse in electrical power system networks using a new voltage stability index," *Int. J. Appl. Eng. Res.*, vol. 12, no. 2, pp. 190–199, 2017.

[113] K. Seethalekshmi, S. N. Singh, and S. C. Srivastava, "Adaptive scheme for minimal load shedding utilizing synchrophasor measurements to ensure frequency and voltage stability," *Electric Power Compon. Syst.*, vol. 38, no. 11, pp. 1211–1227, Aug. 2010, doi: 10.1080/15325001003652884.

[114] Y. Kataoka, M. Watanabe, and S. Iwamoto, "A new voltage stability index considering voltage limits," in *Proc. IEEE PES Power Syst. Conf. Exposit.*, Dec. 2006, pp. 1878–1883, doi: 10.1109/PSCE.2006.296199.

[115] M. T. Tran, "Definition and implementation of voltage stability indices in PSS/ NETOMAC," Chalmers Univ. Technol., Göteborg, Sweden, Tech. Rep. 16035488, 2009.

[116] S. Mohammed, A. H. Eltom, and A. Karrar, "Improved computations of the voltage collapse point," in *Proc. IEEE Power Energy Soc. Gen. Meeting (PESGM)*, Aug. 2019, pp. 1–5, doi: 10.1109/PESGM40551.2019.8973663.

[117] S. Yari and H. Khoshkhoo, "An effective corrective remedial action algorithm to prevent voltage instability," in *Proc. 5th Conf. Knowl. Based Eng. Innov. (KBEI)*, Feb. 2019, pp. 460–466, doi: 10.1109/KBEI.2019.8734950.

[118] P. Akbarzadeh Aghdam and H. Khoshkhoo, "Voltage stability assessment algorithm to predict power system loadability margin," *IET Gener., Transmiss. Distribution*, vol. 14, no. 10, pp. 1816–1828, May 2020, doi: 10.1049/iet-gtd.2019.0230.

[119] M. Kazeminejad, M. Banejad, U. D. Annakkage, and N. Hosseinzadeh, "Load pattern-based voltage stability analysis in unbalanced distribution networks considering maximum penetration level of distributed generation," *IET Renew. Power Gener.*, vol. 14, no. 13, pp. 2517–2525, Oct. 2020, doi: 10.1049/iet-rpg.2019.1196.

[120] K. Alzaareer, M. Saad, H. Mehrjerdi, C. Z. El-Bayeh, D. Asber, and S. Lefebvre, "A new sensitivity approach for preventive control selection in real-time voltage stability assessment," *Int. J. Electr. Power Energy Syst.*, vol. 122, Nov. 2020, Art. no. 106212, doi: 10.1016/j.ijepes.2020.106212.

[121] S. S. Parihar and N. Malik, "Optimal allocation of renewable DGs in a radial distribution system based on new voltage stability index," *Int. Trans. Electr. Energy Syst.*, vol. 30, no. 4, pp. 1–19, Apr. 2020, doi: 10.1002/2050-7038.12295.

[122] J. Jung, H. Cho, B. Park, S. Nam, K. Hur, and B. Lee, "Enhancement of linearity and constancy of PMU-based voltage stability index: Application to a Korean wide-area monitoring system," *IET Gener., Transmiss. Distribution*, vol. 14, no. 17, pp. 3357–3364, Sep. 2020, doi: 10.1049/iet-gtd.2019.0773.

[123] S. K. Gupta, S. K. Mallik, D. Kumar, and S. Kumar, "Voltage stability assessment of the power system using novel line voltage collapse index," *Eng. Res. Express*, vol. 6, no. 2, May 2024, Art. no. 025324, doi: 10.1088/2631-8695/ad4254.

[124] M. Calin, A. M. Dumitrescu, M. Asprou, E. Kyriakides, and M. Albu, "Measurement data aggregation for active distribution networks," in *Proc. IEEE Int. Workshop Appl. Meas. Power Syst. (AMPS)*, Sep. 2013, pp. 144–149, doi: 10.1109/AMPS.2013.6656241.

[125] T. Van Cutsem, M. Glavic, W. Rosehart, C. Canizares, M. Kanatas, L. Lima, F. Milano, L. Papangelis, R. A. Ramos, J. A. d. Santos, B. Tamimi, G. Taranto, and C. Vournas, "Test systems for voltage stability studies," *IEEE Trans. Power Syst.*, vol. 35, no. 5, pp. 4078–4087, Sep. 2020.